

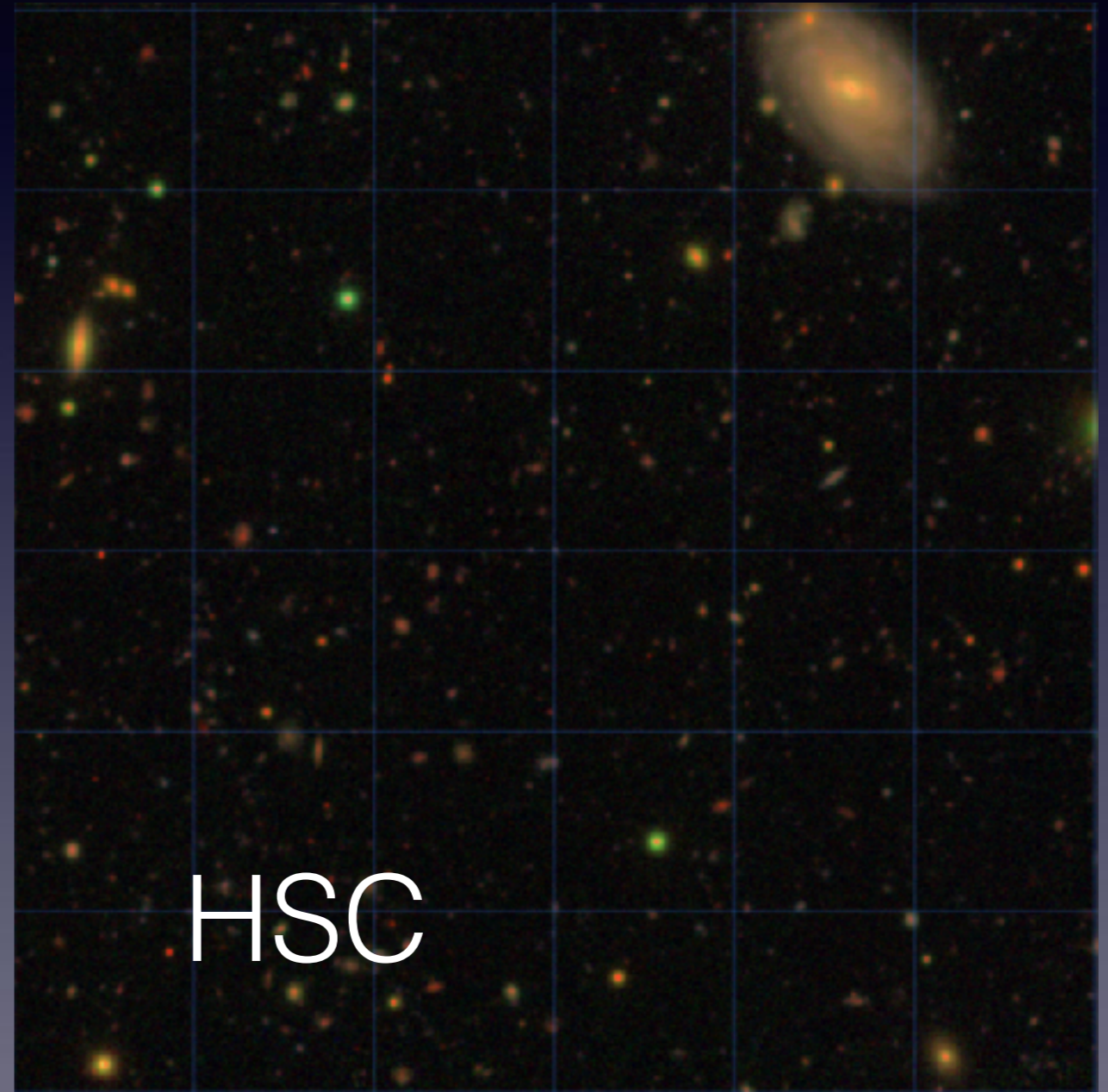
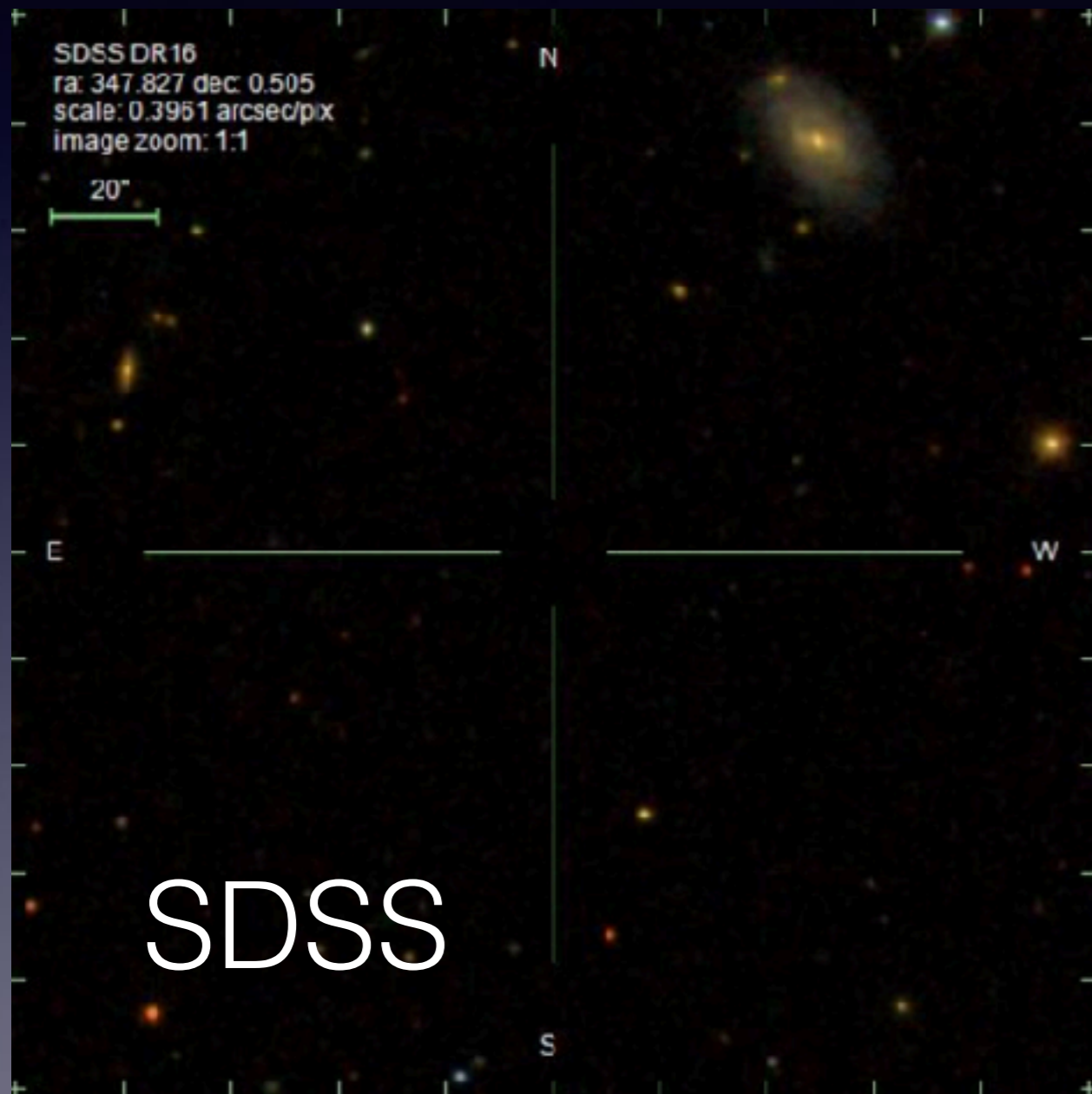
Towards ZTF-III

Nao Suzuki (Lawrence Berkeley National Lab / LPNHE)

- Multi SN Species (SNIb, SNIc, SNIId)
- Probing Dark Galaxies
- RR Lyrae, Cepheid Variables (DESI-II Spectra)
- Mapping the local Universe

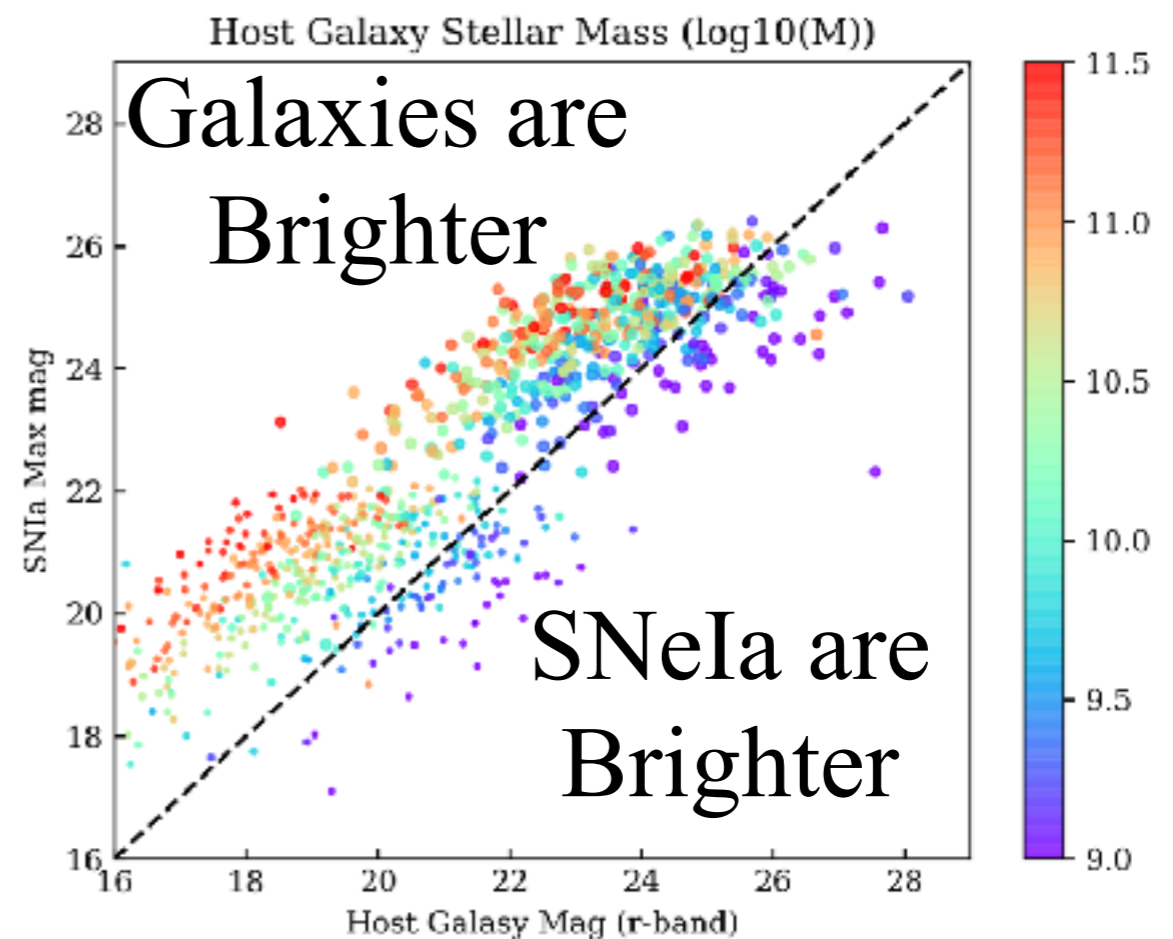
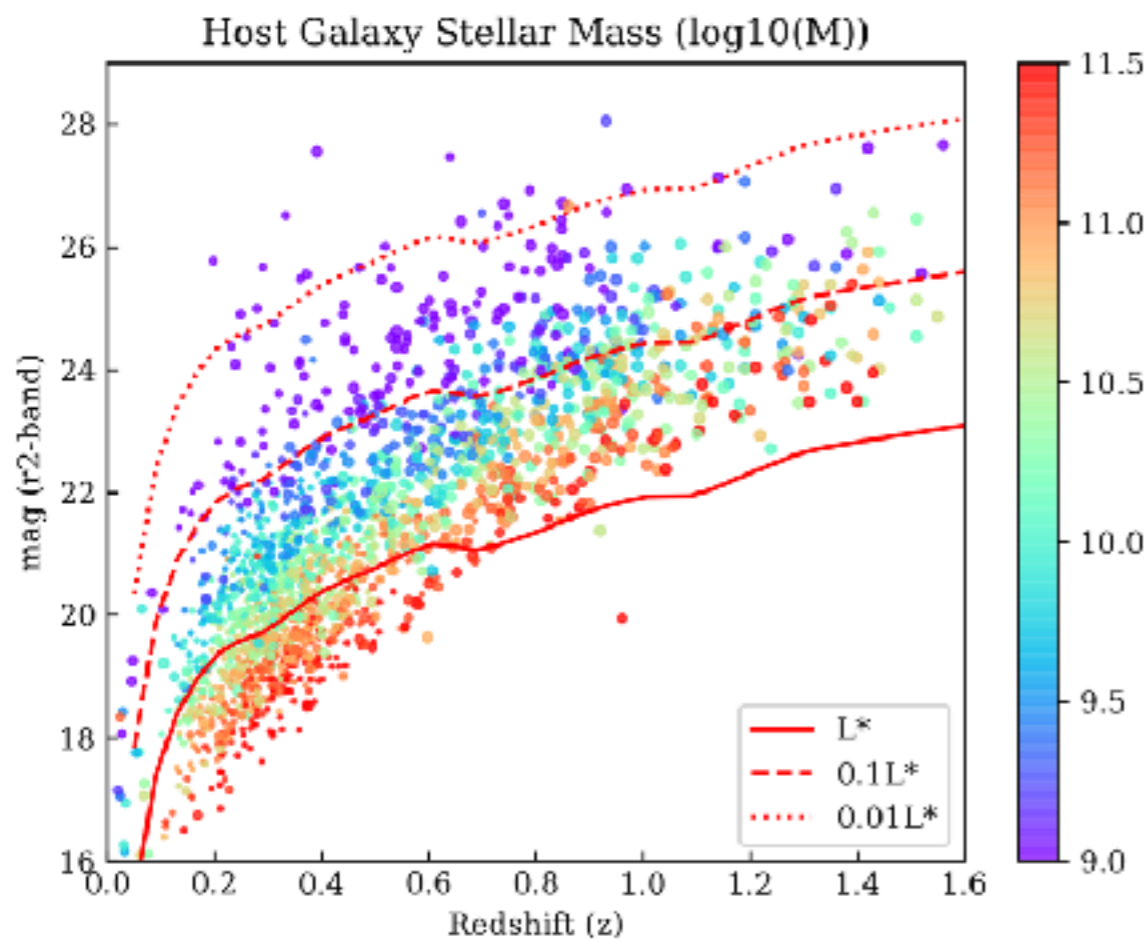
Probing “Dark” galaxies (1/3)

ZTF × LSST (Subaru/HSC)



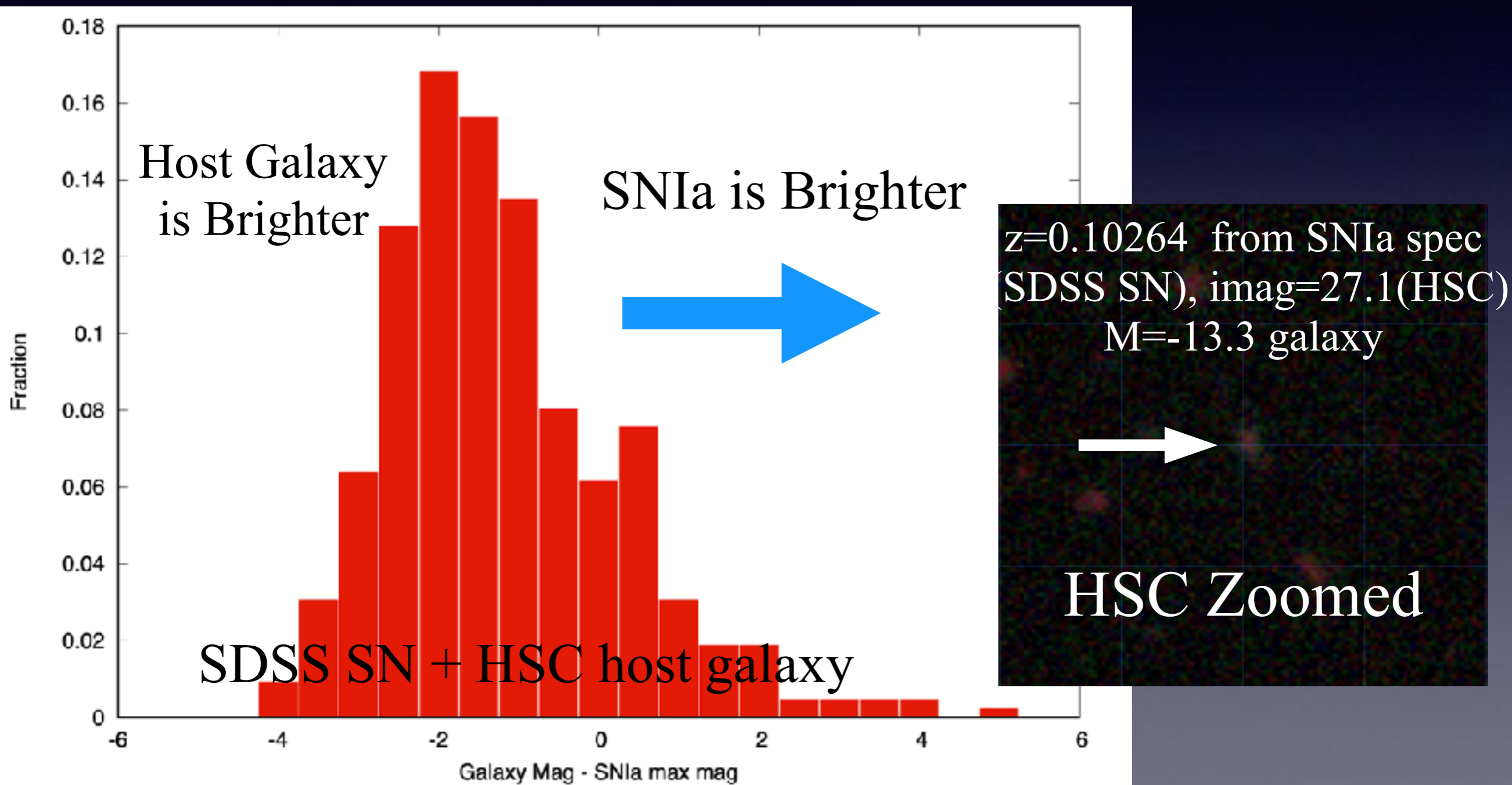
Probing “Dark” galaxies (2/3)

ZTF × LSST (Subaru/HSC)



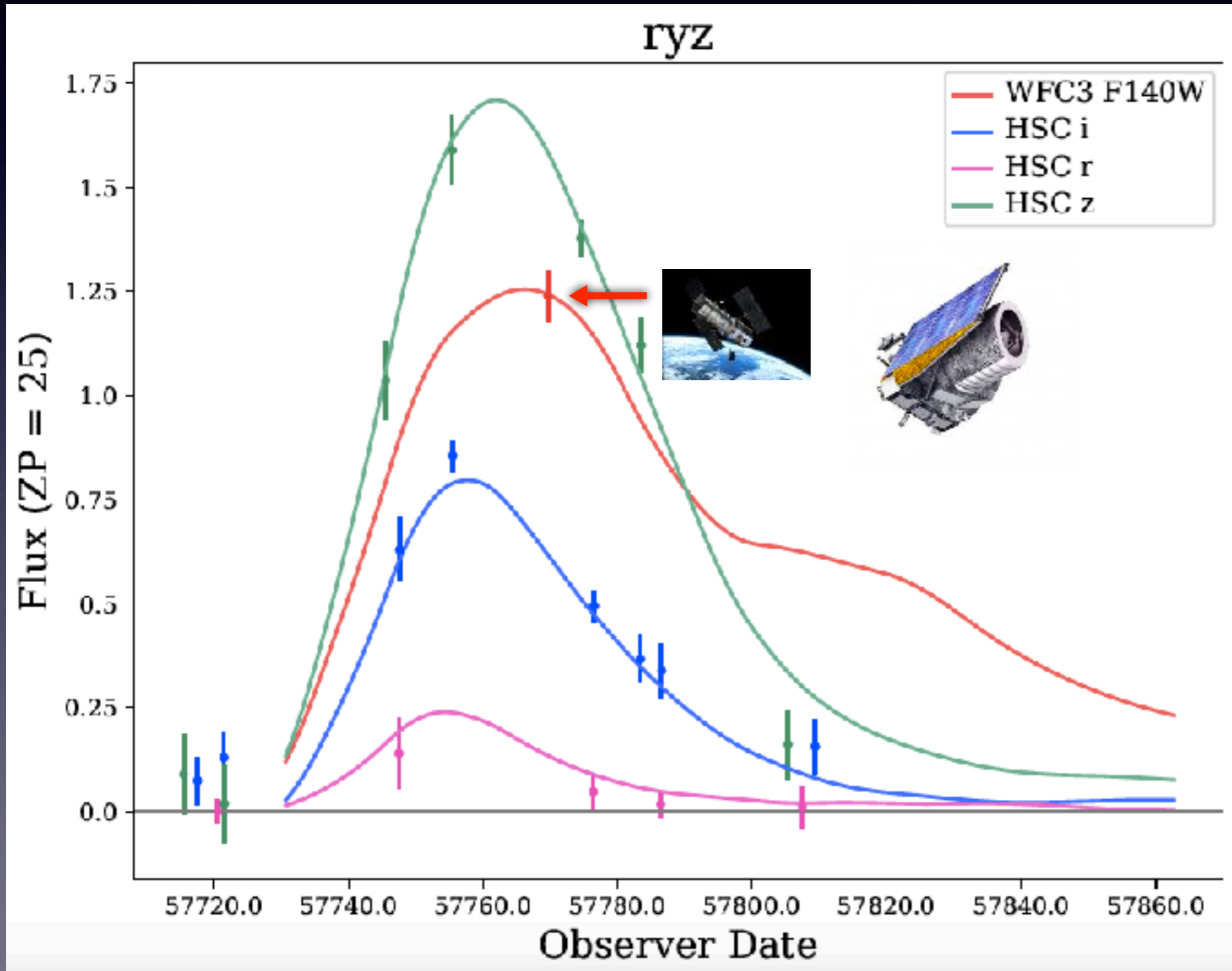
Probing “Dark” galaxies (3/3)

ZTF × LSST (Subaru/HSC)



Probing IR with Euclid

ZTF x Euclid (Image + Spec)



Euclid : J, H, K

Euclid : IR Spec

Schedule is fixed

for next 6 years

ZTF-III start
observing Euclid
field 2 weeks in
advance

Pre-ZTF Meeting in Japan 2019

TDA-MMS 2019: Time Domain Astronomy in the Era of Massively Multiplexed Spectroscopy

February 8-10, 2019, Nikko, Japan



Distribution of Local Matter on BAO Scale

Nao Suzuki & Friends

A visualization of the cosmic web, showing a complex network of filaments and nodes. The filaments are colored in shades of purple and blue, while the nodes are highlighted in bright yellow and orange. The overall structure is a dense, interconnected web of matter.

Q Where are we?

Hubble's Law

$$v = H_0 d$$

v = recession velocity in km/sec

d = distance in Mpc

H_0 = expansion rate today (*Hubble Parameter*)

In words:

The more *distant* a galaxy, the *faster* its recession velocity.

General Relativity Metric

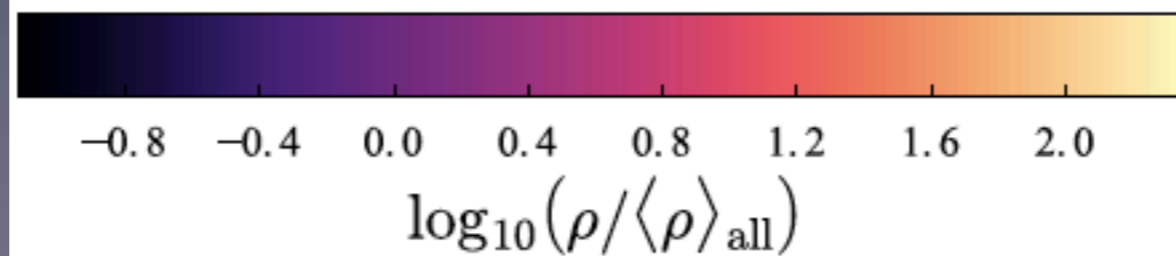
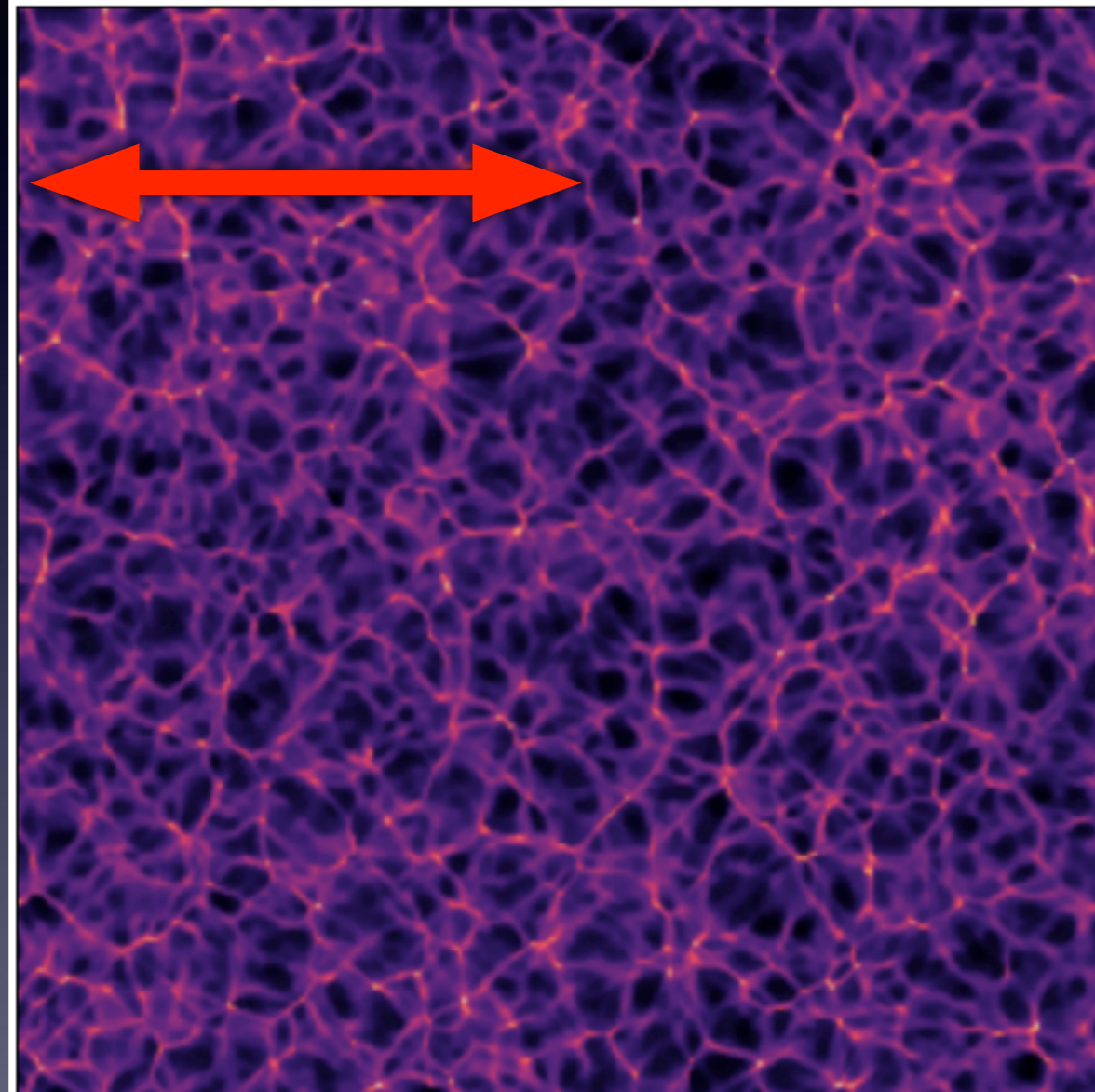
Robertson-Walker Metric

$$ds^2 = dt^2 - \frac{R^2(t)}{c^2} \left[\frac{dr^2}{1 - kr^2} + r^2 d\theta^2 + r^2 \sin^2 \theta d\phi^2 \right]$$

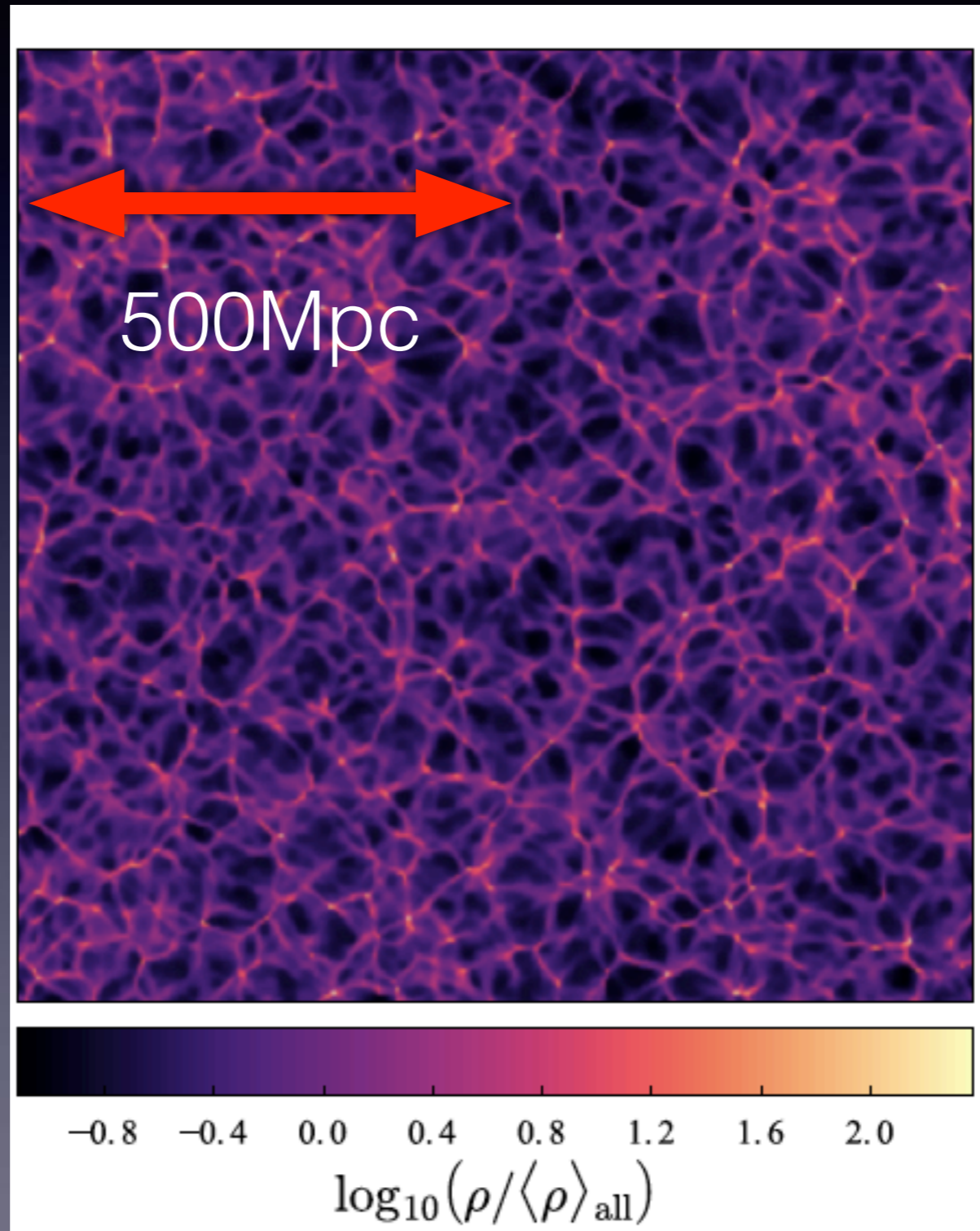
Schwartzschild Metric

$$ds^2 = \left(1 - \frac{2m}{r} \right) dt^2 - \frac{dr^2}{1 - \frac{2m}{r}} - r^2 d\theta^2 - r^2 \sin^2 \theta d\phi^2$$

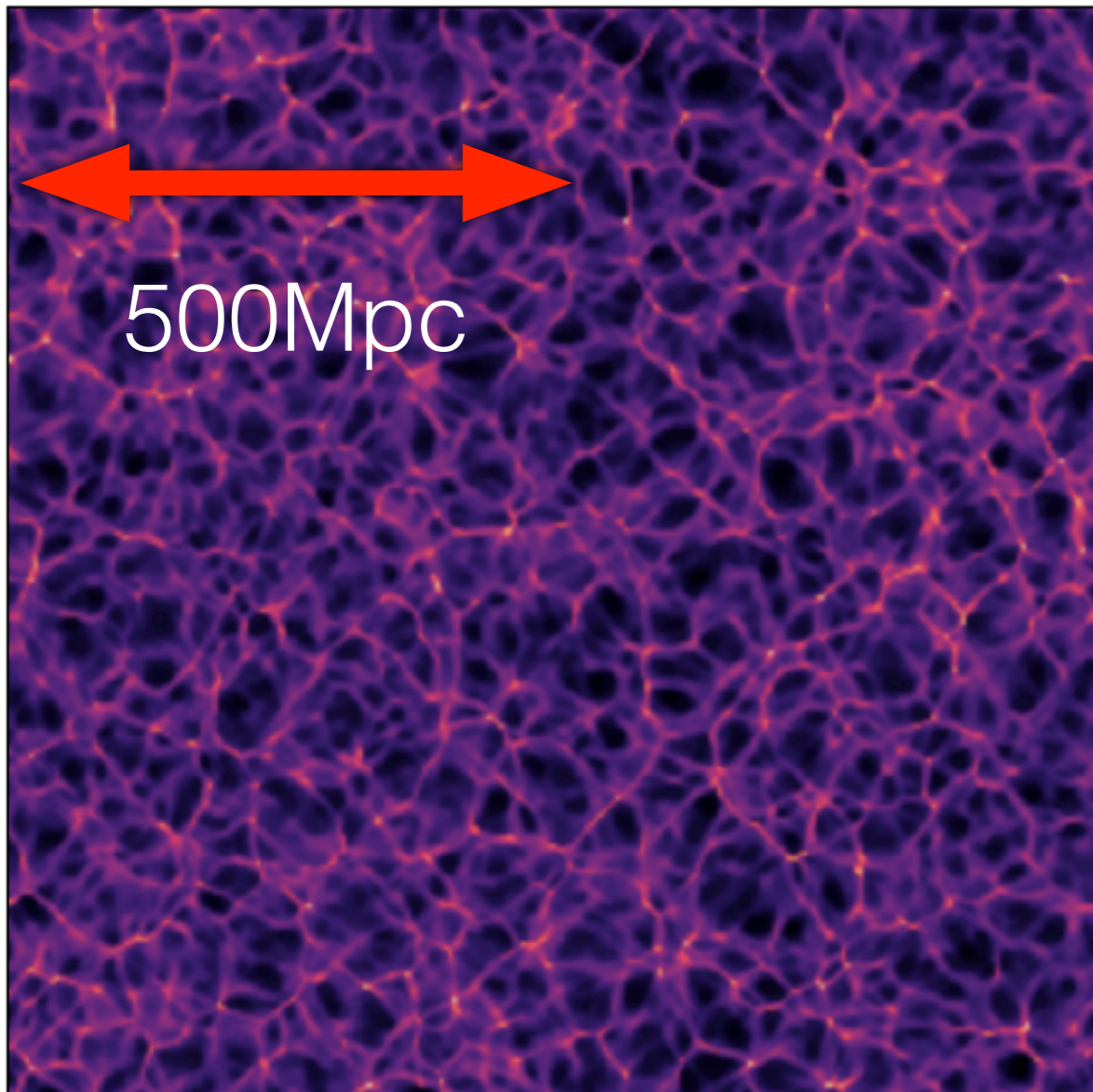
Density Field at $z=0$



Density Field at $z=0$

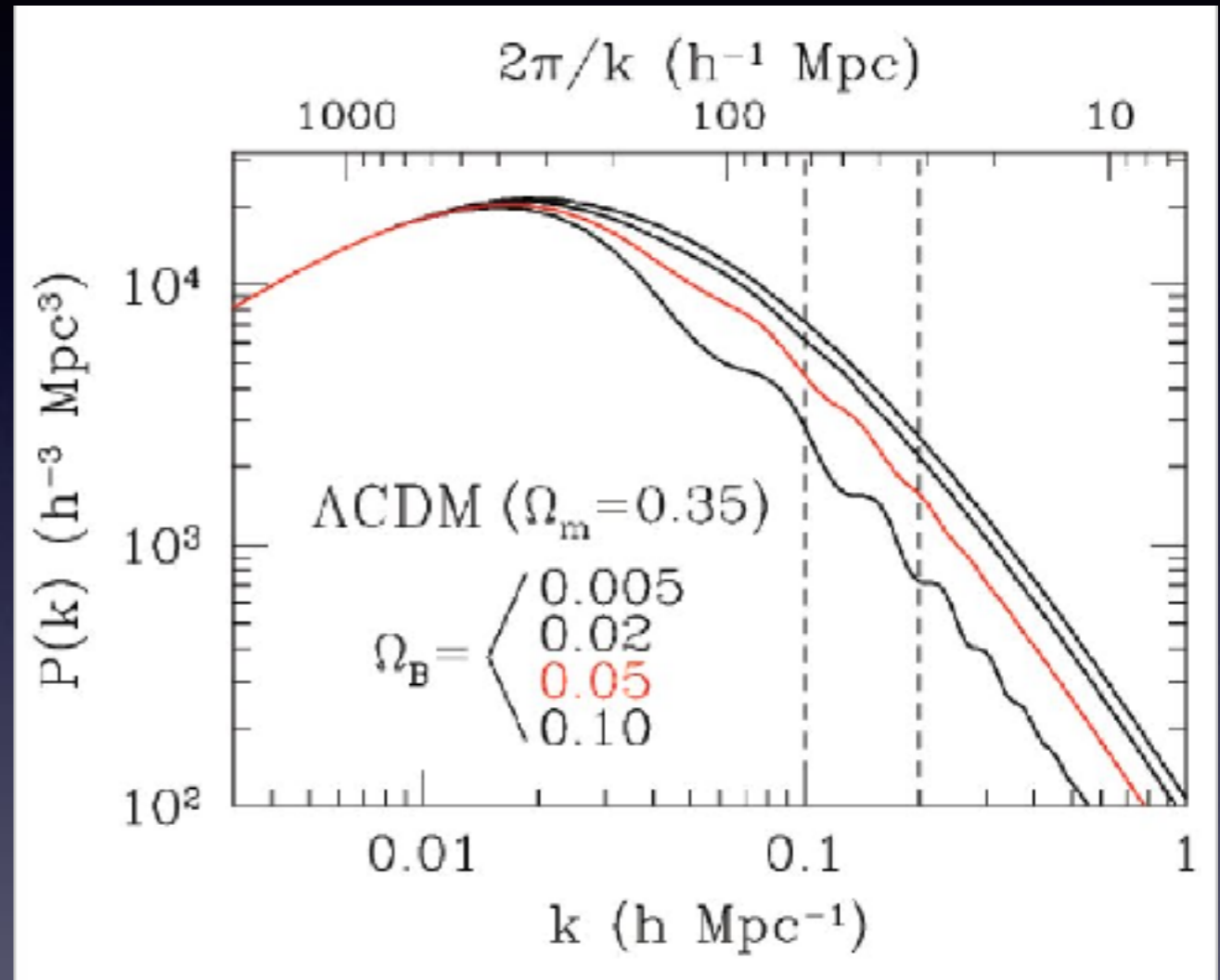


How to quantify density fluctuation?



-0.8 -0.4 0.0 0.4 0.8 1.2 1.6 2.0

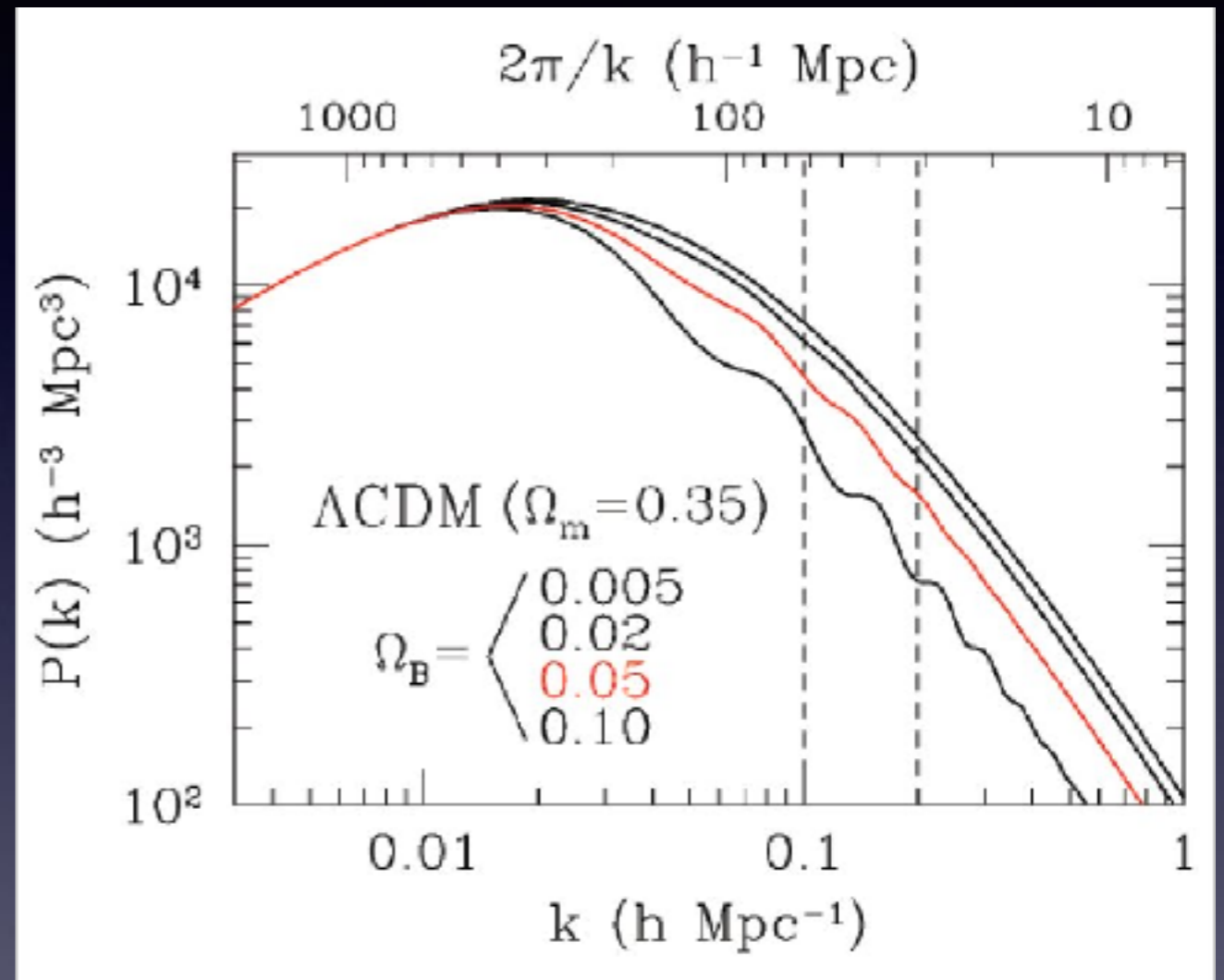
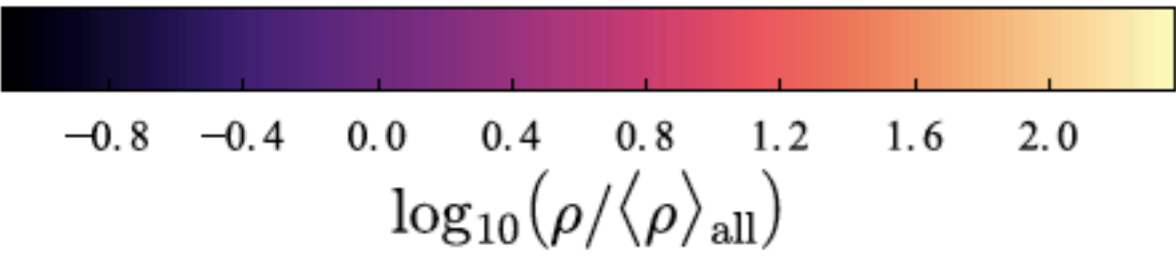
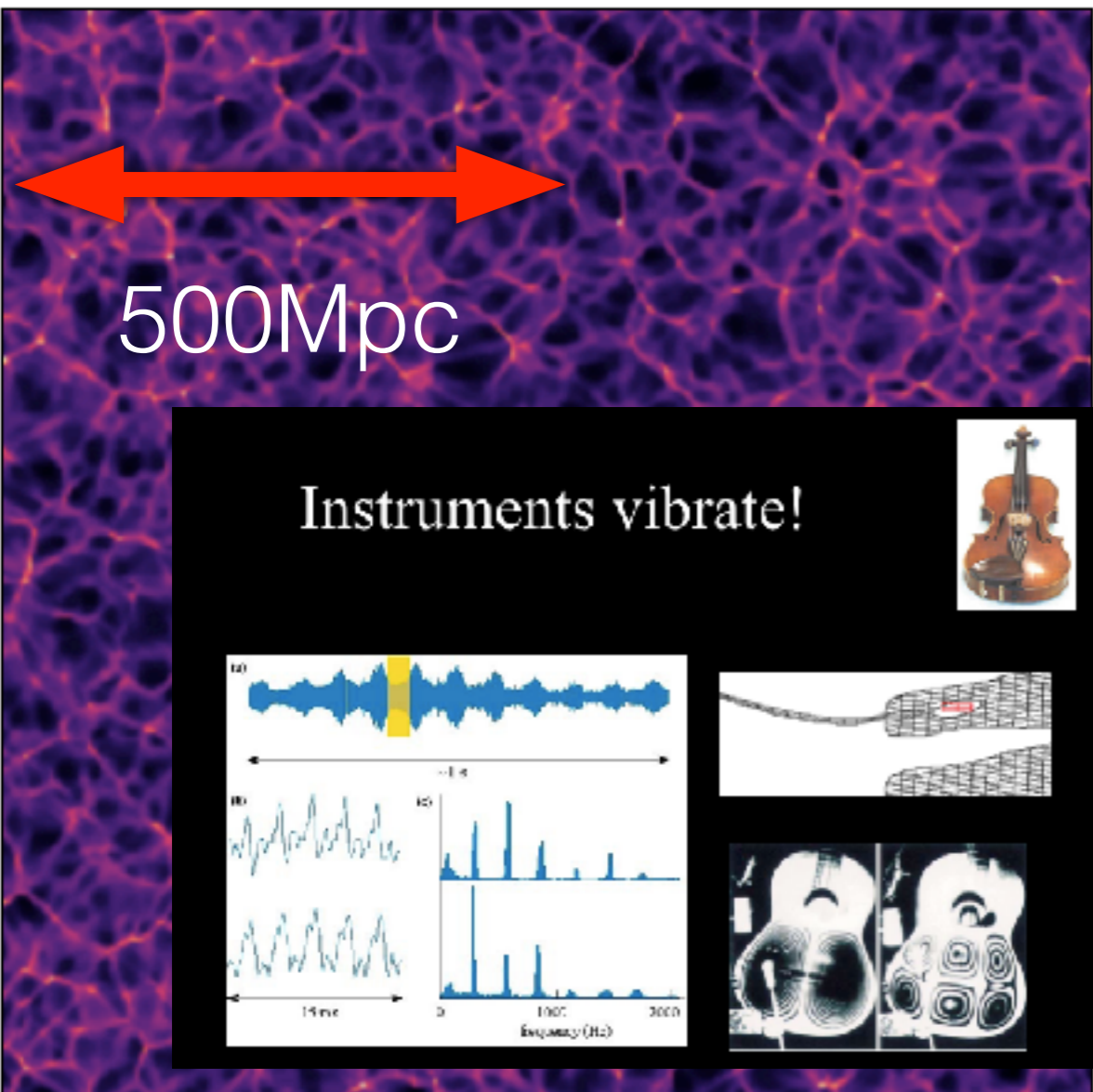
$\log_{10}(\rho/\langle\rho\rangle_{\text{all}})$



Einj said: ↑

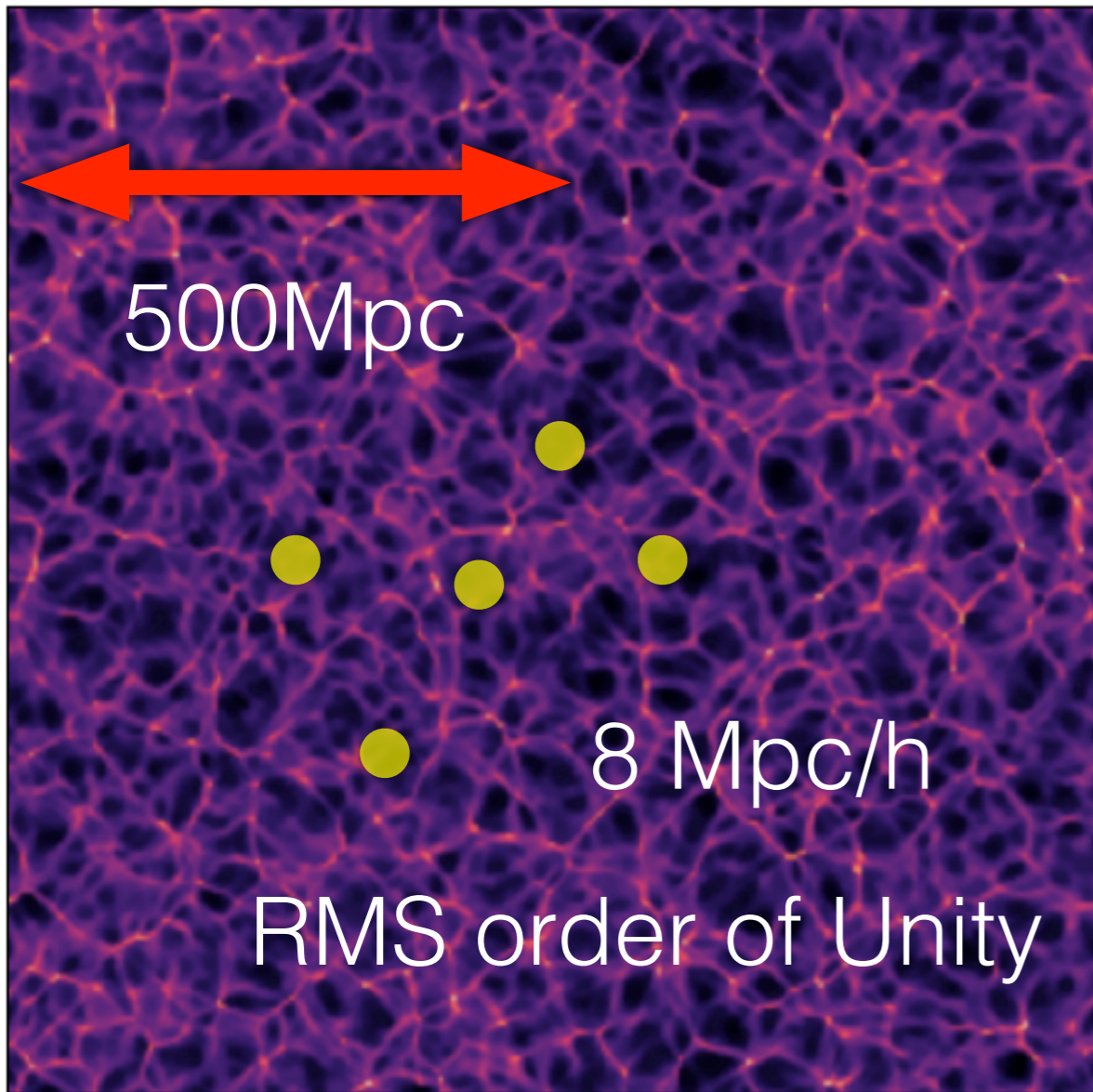
Thanks a lot! Does that simply mean $\sigma_8 = \mathcal{P}(k = 1/8 h/\text{Mpc})$? Where \mathcal{P} is the power spectrum.

Harmonics has to be counted Window Function $W(kR)$

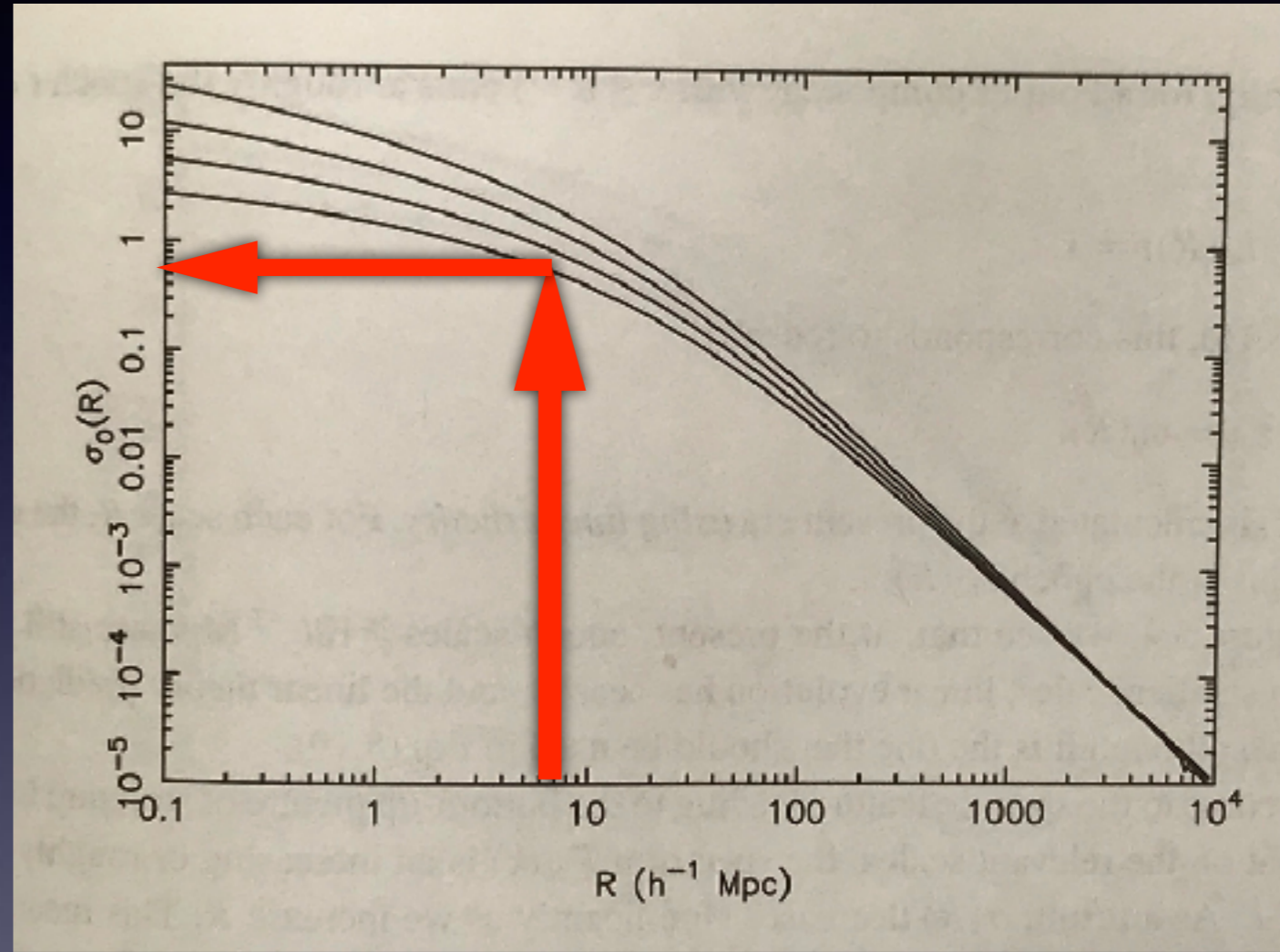


$$\sigma_0^2(R) = \int_0^\infty W^2(kR) \left(\frac{k}{a_0 H_0}\right)^4 T^2(k) \delta_H^2(k) \frac{dk}{k}$$

8 Mpc/h : RMS is Unity (0.8-ish)

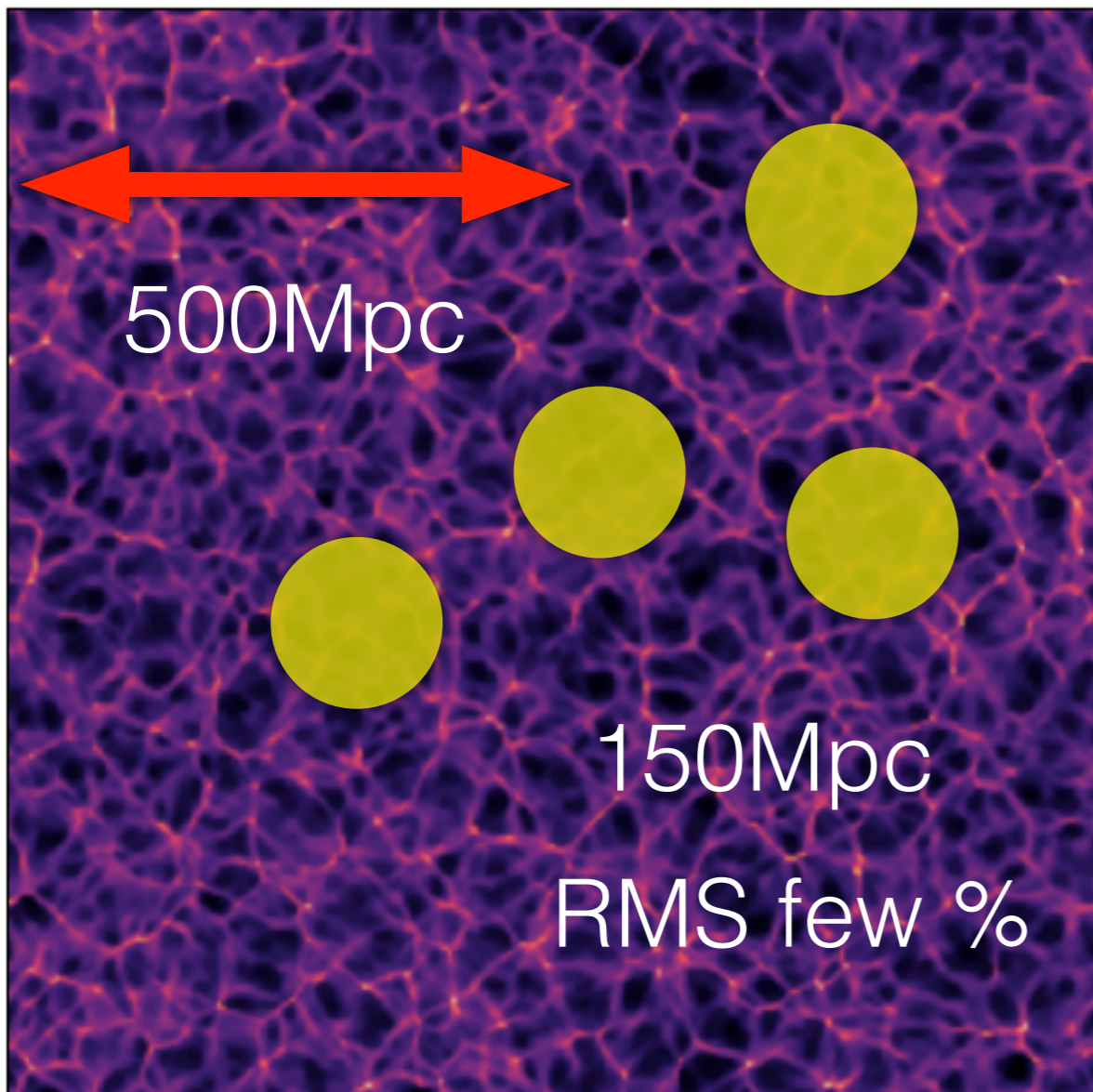


-0.8 -0.4 0.0 0.4 0.8 1.2 1.6 2.0
 $\log_{10}(\rho/\langle\rho\rangle_{\text{all}})$

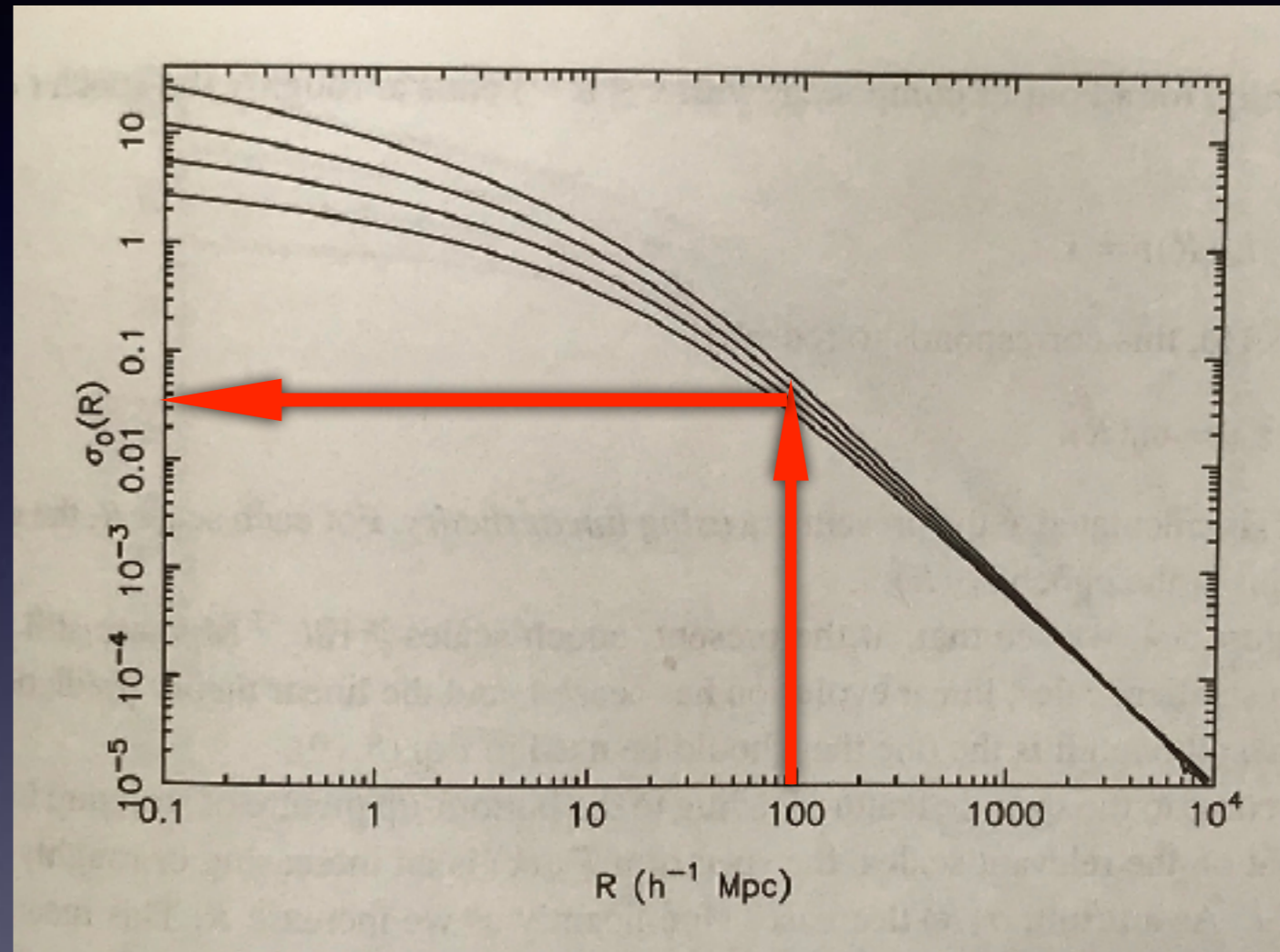


$$\sigma_0^2(R) = \int_0^\infty W^2(kR) \left(\frac{k}{a_0 H_0}\right)^4 T^2(k) \delta_H^2(k) \frac{dk}{k}$$

150Mpc represents the Universe



-0.8 -0.4 0.0 0.4 0.8 1.2 1.6 2.0
 $\log_{10}(\rho/\langle\rho\rangle_{\text{all}})$



$$\sigma_0^2(R) = \int_0^\infty W^2(kR) \left(\frac{k}{a_0 H_0}\right)^4 T^2(k) \delta_H^2(k) \frac{dk}{k}$$

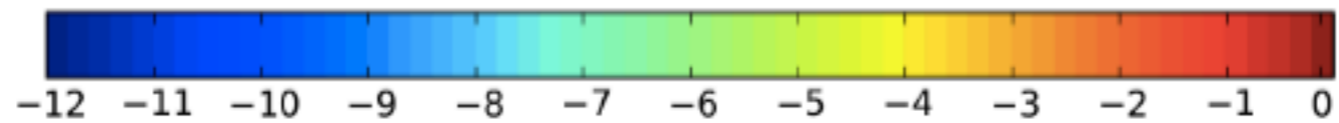
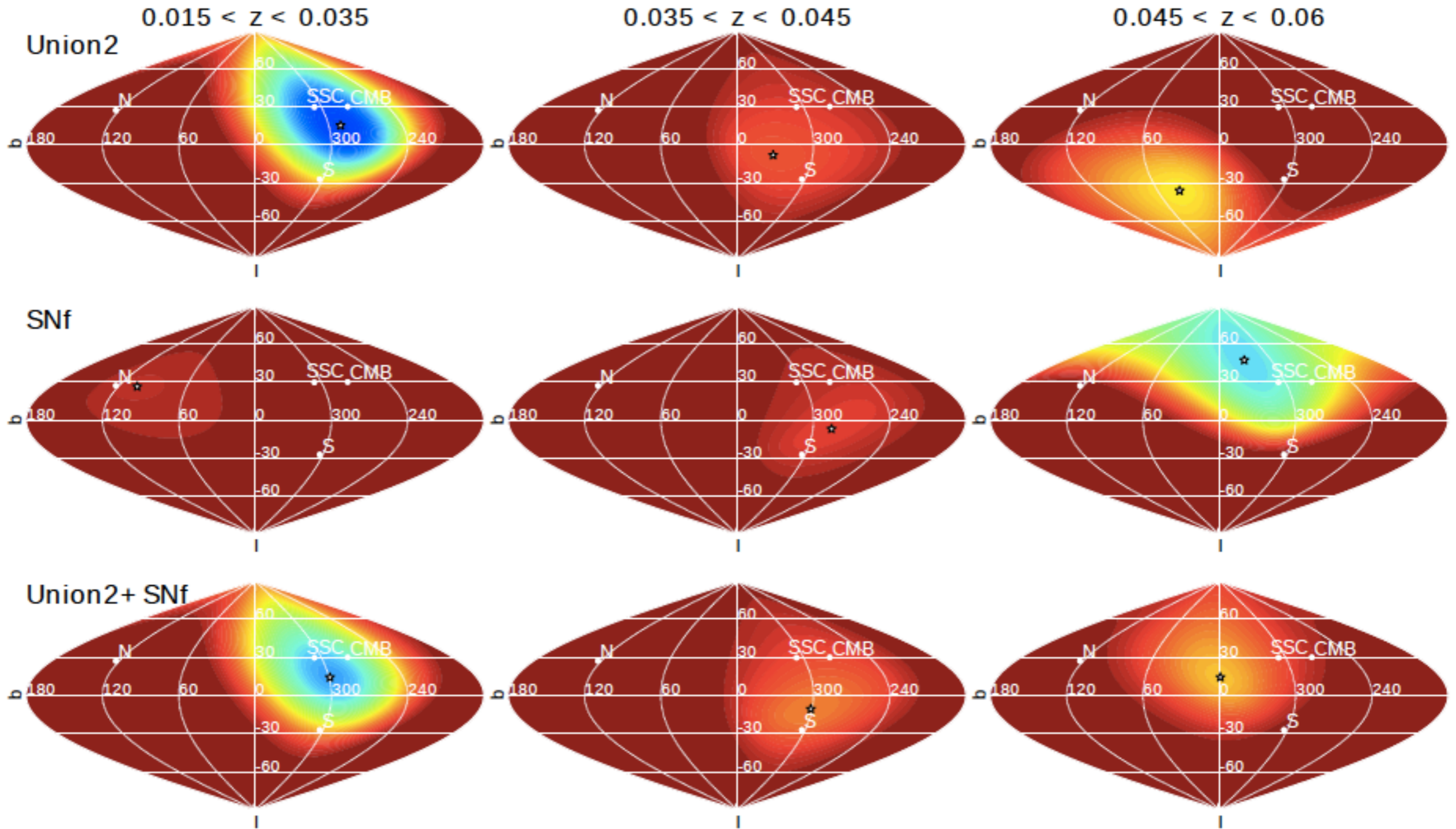
Q What is the area to study for 150Mpc?

Q1 : $z=2$

Q2 : $z=0$

CMB Dipole is seen by SNIa

A&A 560, A90 (2013)



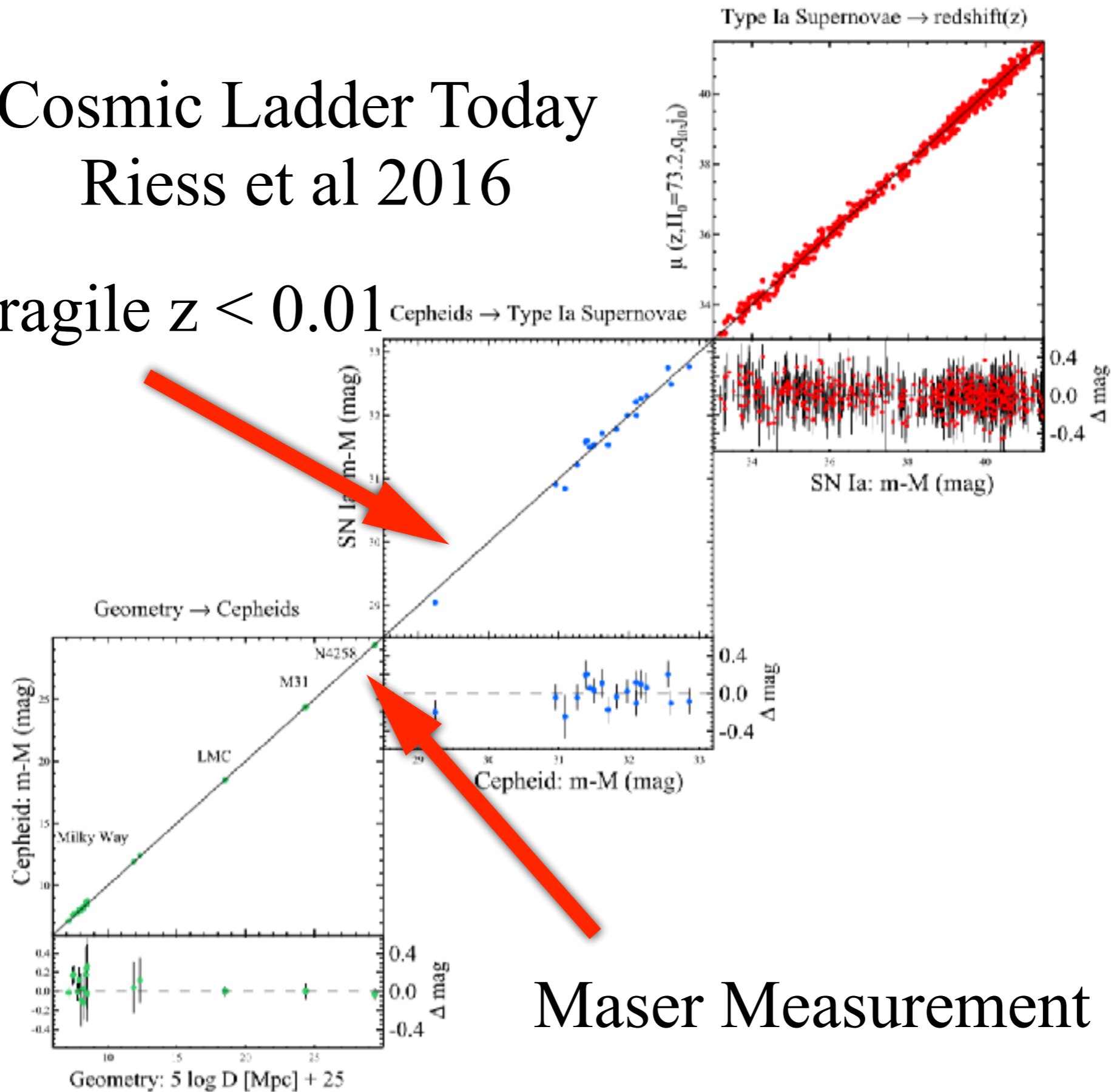
$\gamma^2 - \gamma^2 (v=0)$

Feindt et al. 2011

Cosmic Ladder Today

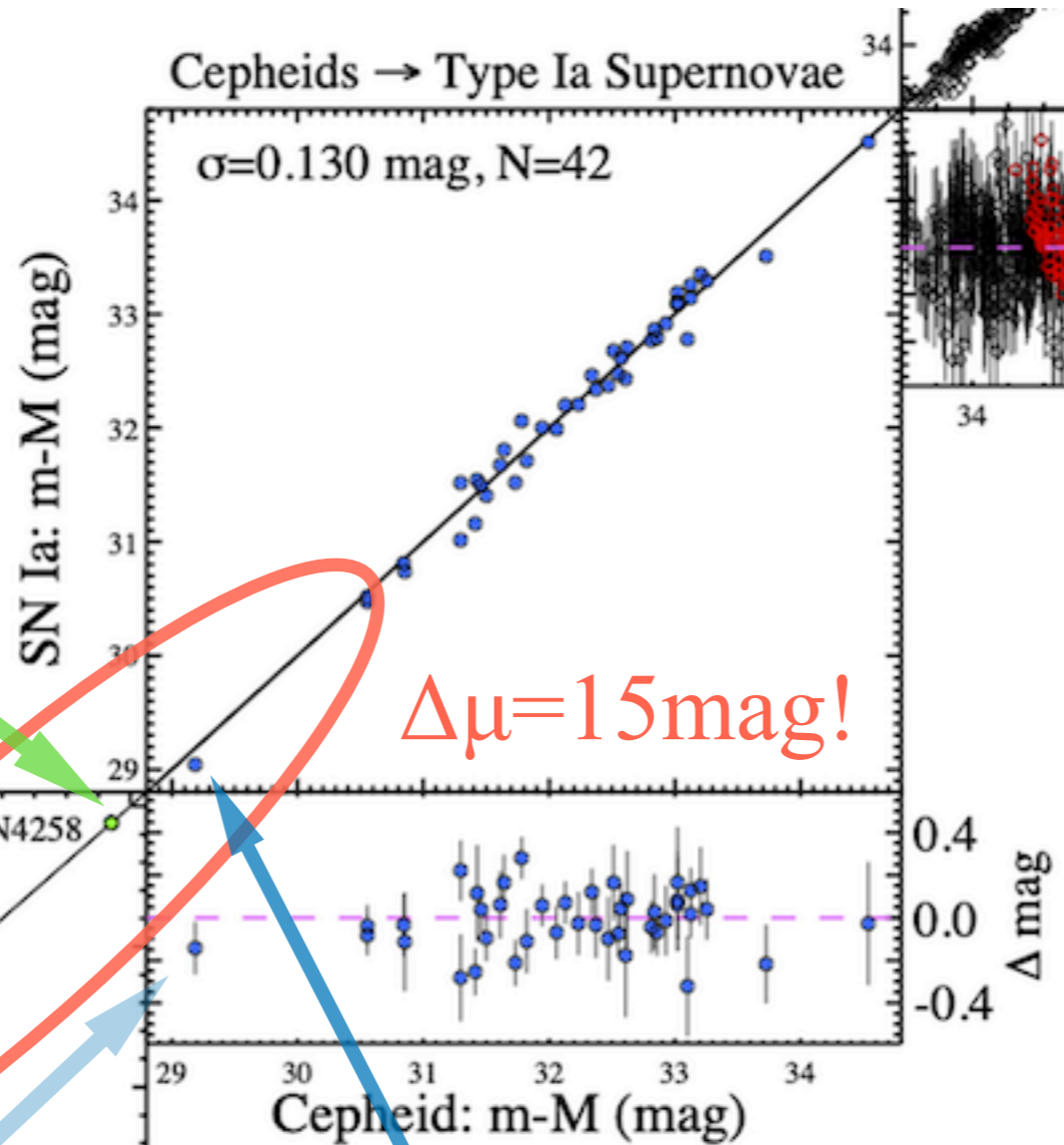
Riess et al 2016

Fragile $z < 0.01$ Cepheids \rightarrow Type Ia Supernovae





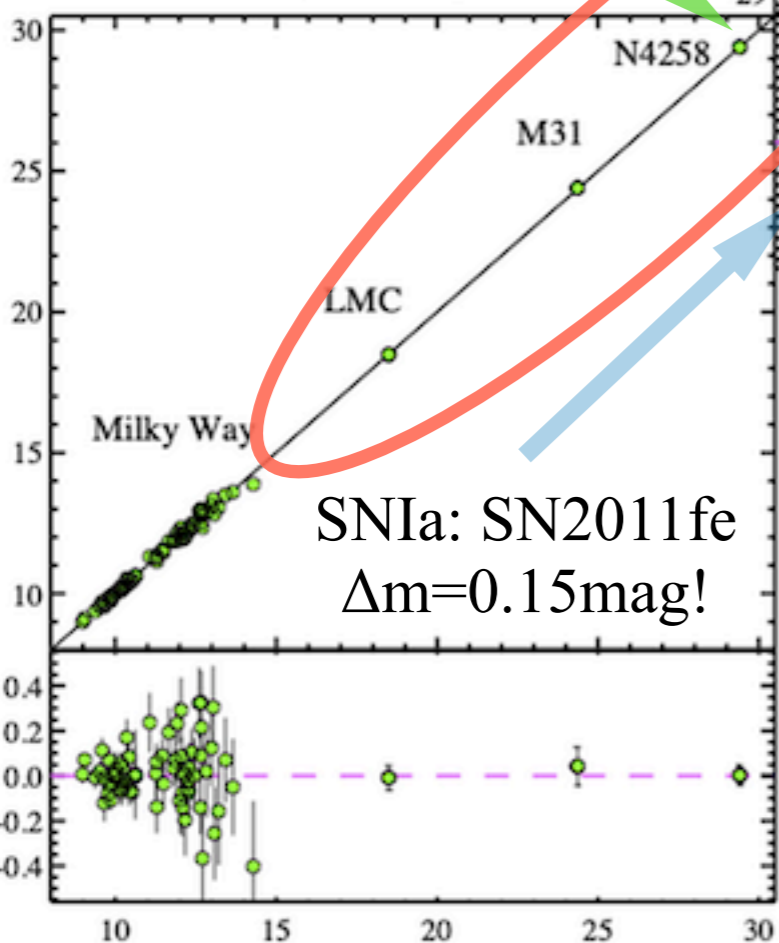
NGC4258



$\Delta\mu=15\text{mag!}$

Cepheid: m-M (mag)

Geometry -> Cepheids



SNIa: SN2011fe
 $\Delta m=0.15\text{mag!}$

M101



Riess et al 2022

Geometry: $5 \log D [\text{Mpc}] + 25$

HSC FoV

**Disk+Halo : $5' < \theta < 10'$
($10 < r < 20$ kpc)**

Halo : $\theta > 10'$ ($r > 20$ kpc)

M101

Inhomogeneous Expansion of the Universe

The trouble with Hubble: Local versus global expansion rates in inhomogeneous cosmological simulations with numerical relativity

HAYLEY J. MACPHERSON,¹ PAUL D. LASKY,^{1,2} AND DANIEL J. PRICE¹

¹*Monash Centre for Astrophysics and School of Physics and Astronomy,
Monash University, VIC 3800, Australia*

²*OzGrav: The ARC Centre of Excellence for Gravitational-wave Discovery, Clayton, VIC 3800, Australia*

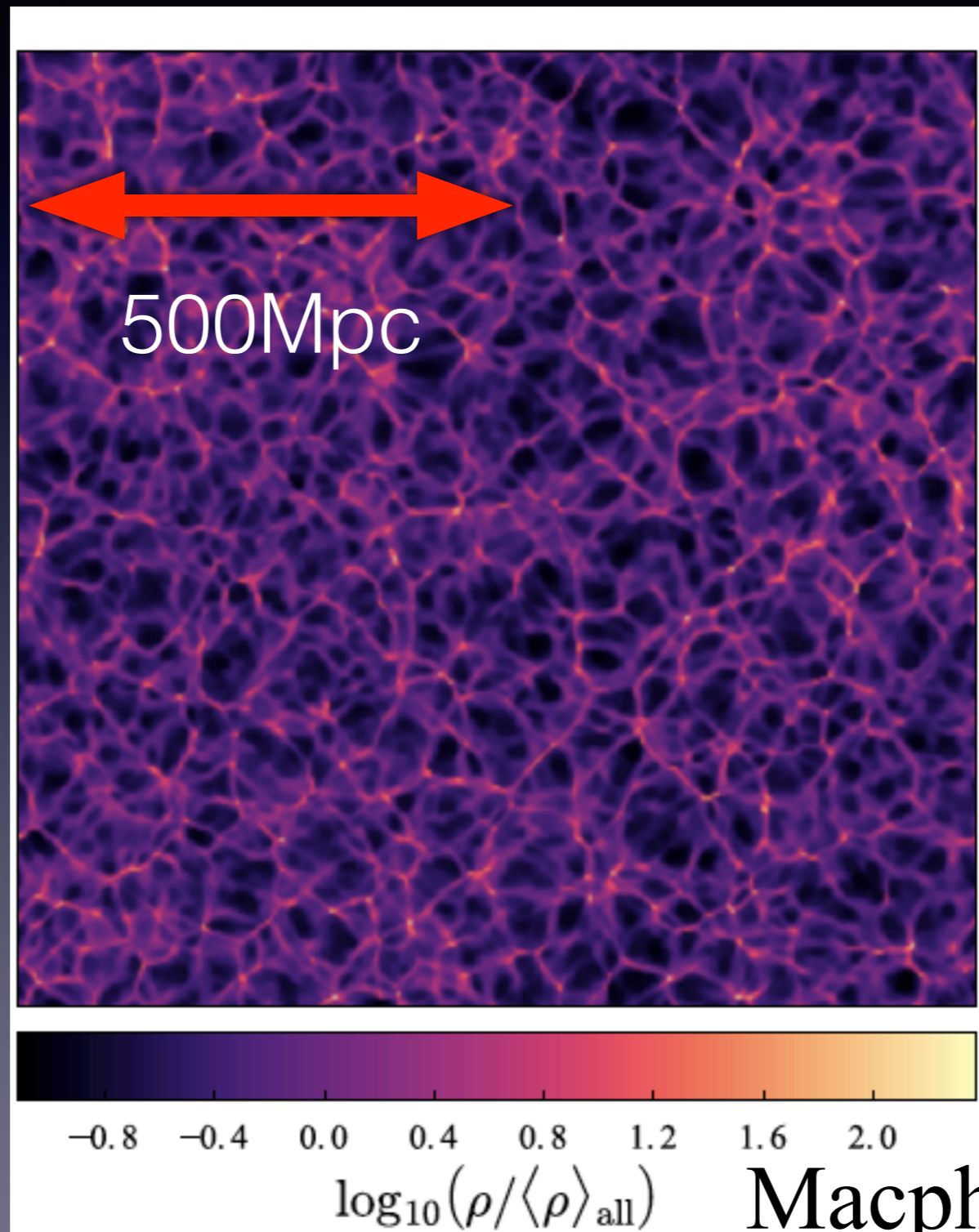
Submitted to ApJ

Macpherson et al 2018

ABSTRACT

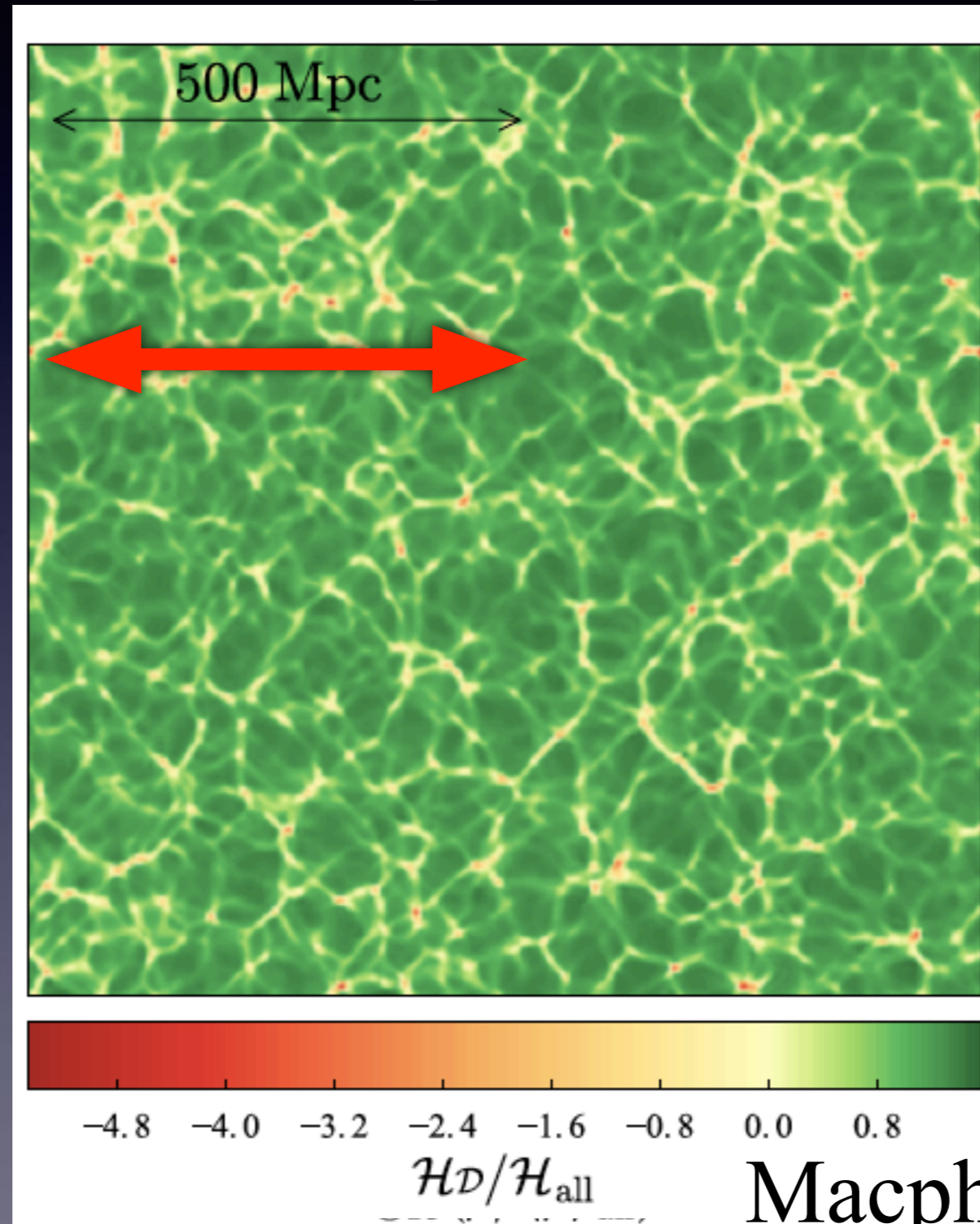
In a fully inhomogeneous, anisotropic cosmological simulation performed by solving Einstein's equations with numerical relativity, we find a local measurement of the effective Hubble parameter differs by less than 1% compared to the global value. This variance is consistent with predictions from Newtonian gravity. We analyse the averaged local expansion rate on scales comparable to Type 1a supernova surveys, and find that local variance cannot resolve the tension between the Riess et al. (2018a) and Planck Collaboration et al. (2018) measurements.

Density Field at $z=0$



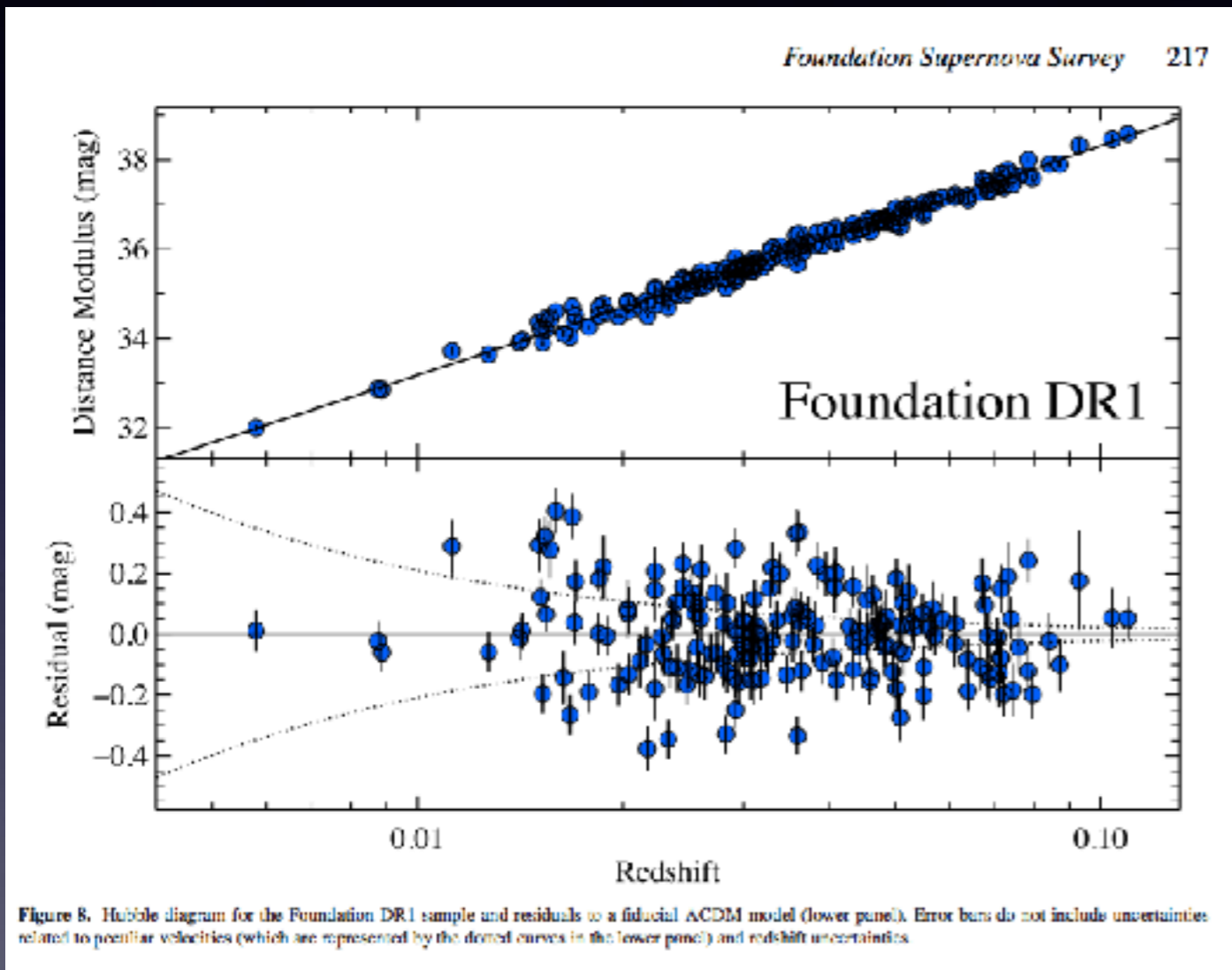
Macpherson et al 2018

Expansion Rate at $z=0$ (normalized by global) Inhomogeneous Expansion of the Universe

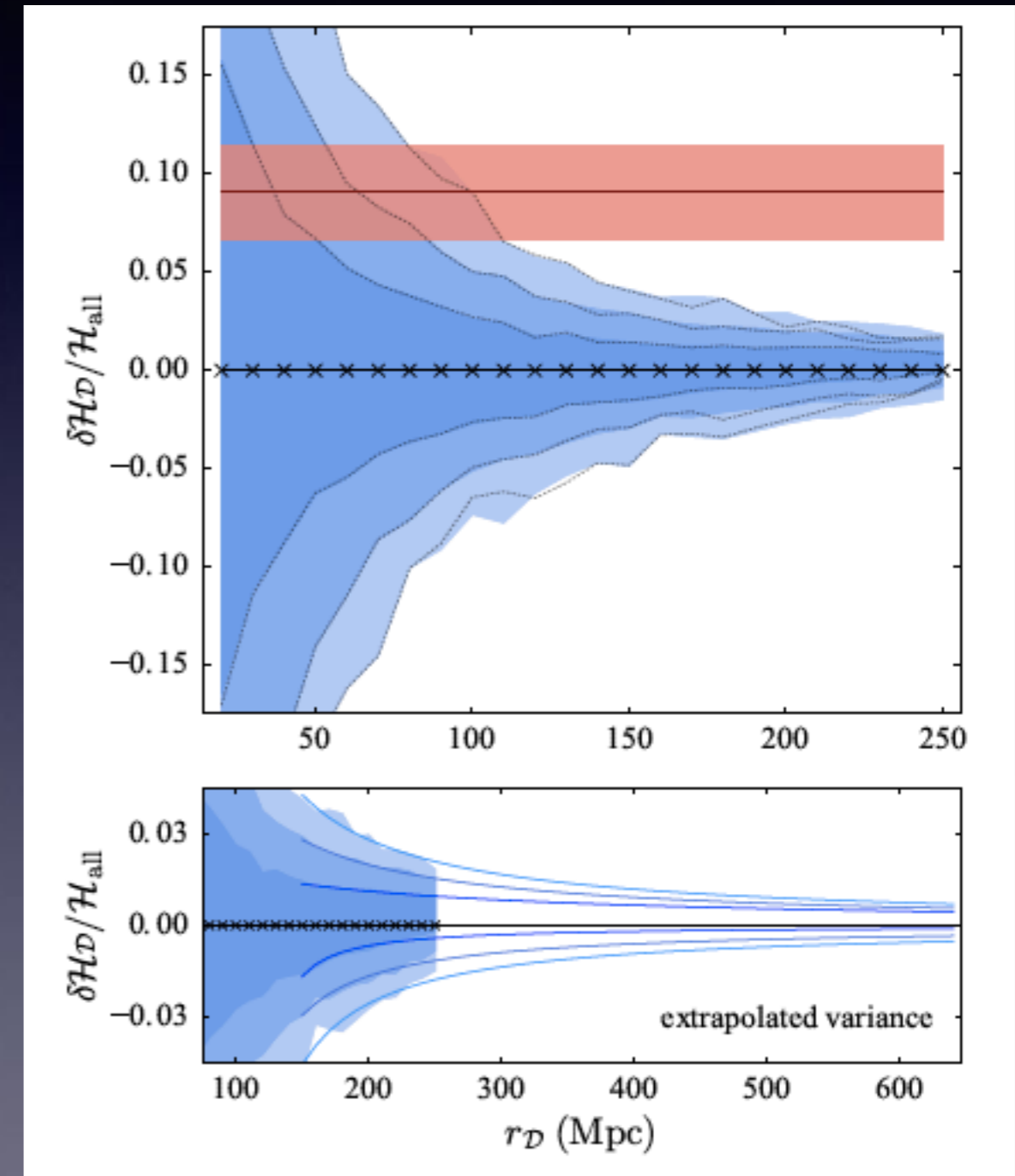


Macpherson et al 2018

Hubble Flow vs SNIa Cosmology



Foley et al 2018



Macpherson et al 2018

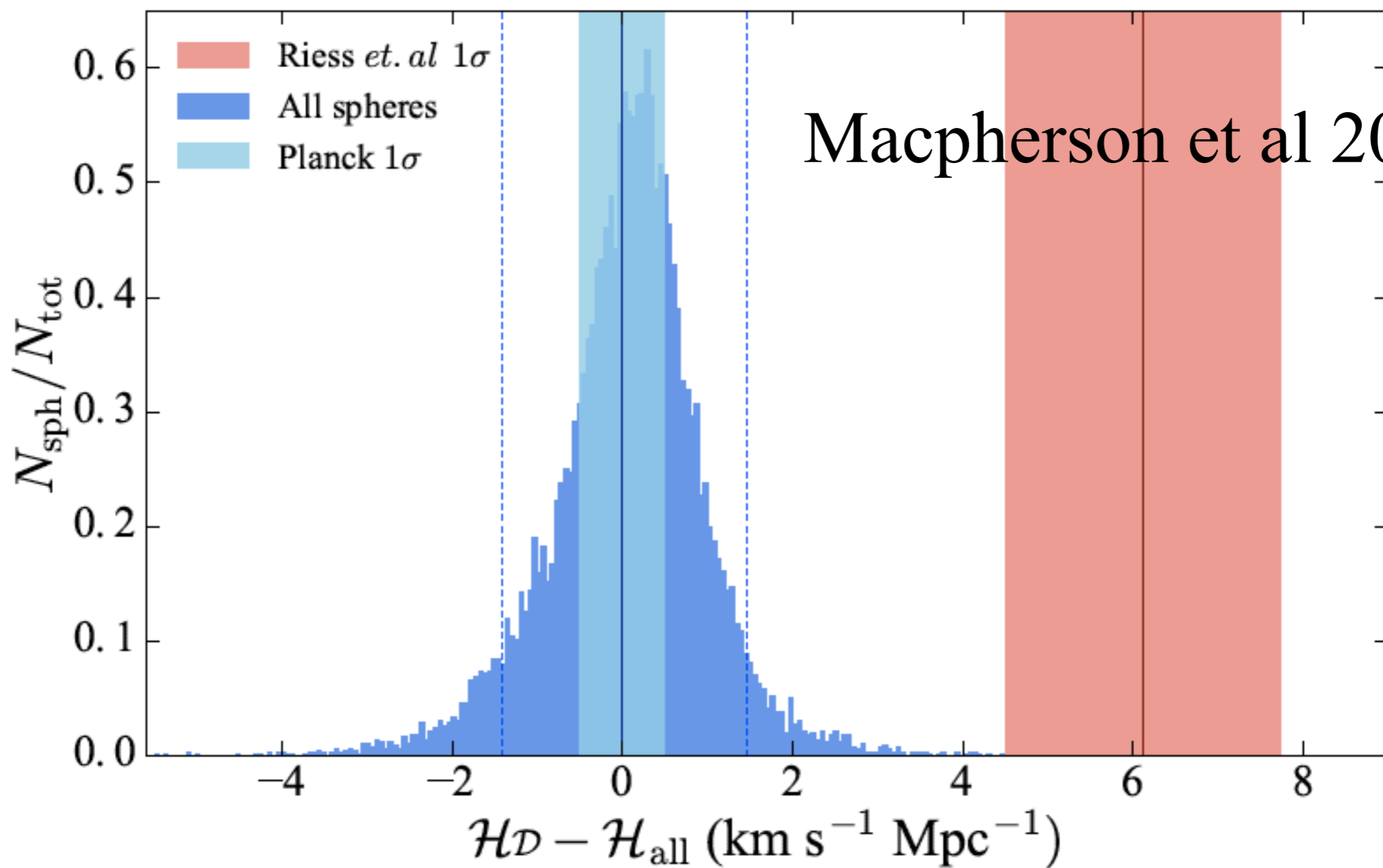


Figure 3. Local deviations in the Hubble parameter due to inhomogeneities. We show the full distribution of all spheres in the range $75 < r_D < 180 h^{-1}$ Mpc in blue. The dashed blue lines represent the 1σ deviation of the inhomogeneous distribution. The blue shaded region represents the 1σ uncertainties on the Planck Collaboration et al. (2016) measurement, while the solid red line and shaded region represent the mean and 1σ deviation in the Riess et al. (2018a) measurement, respectively.

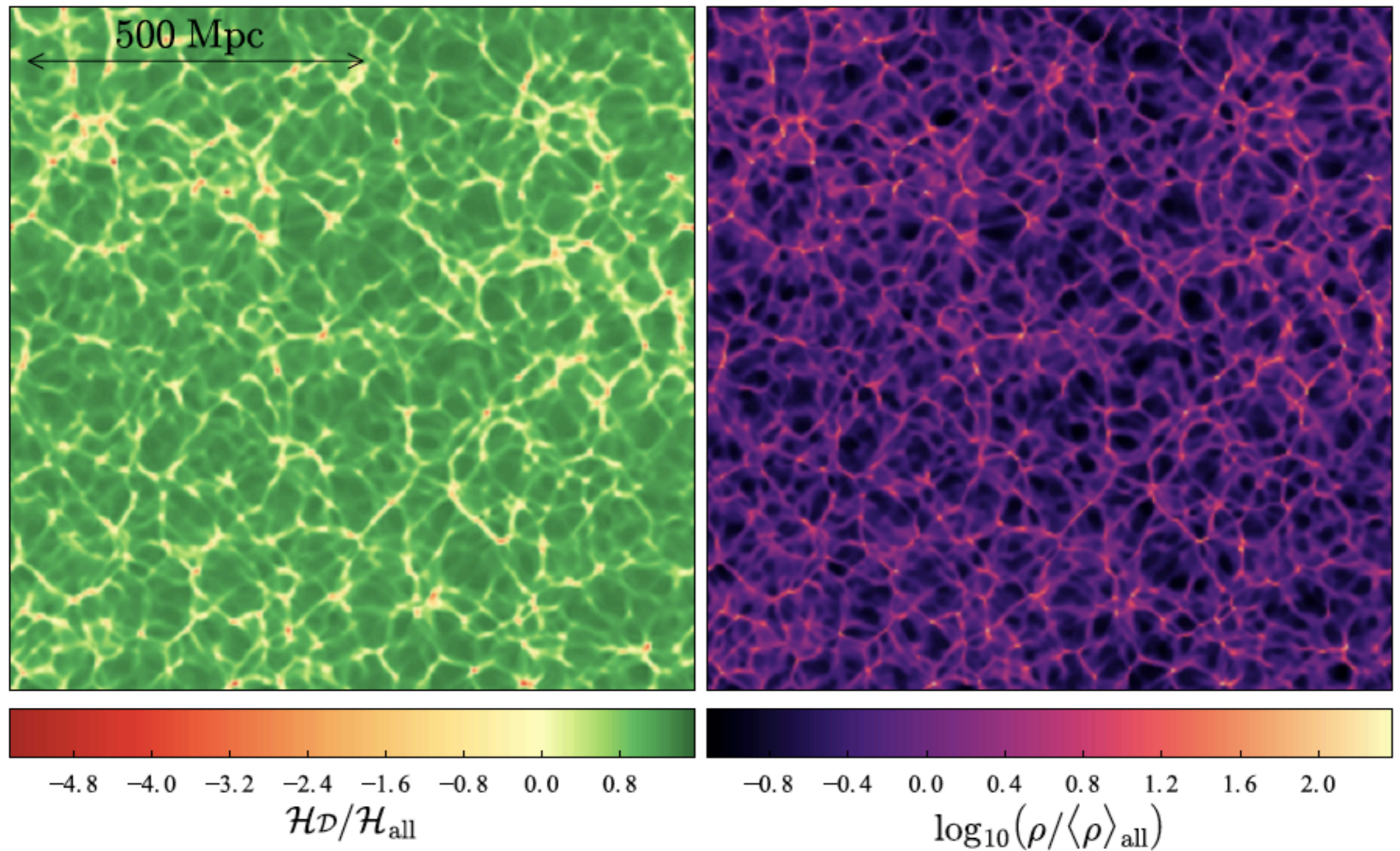


Figure 1. Expansion rate and density of an inhomogeneous, anisotropic universe. Left panel shows the deviation in the Hubble parameter relative to the global mean \mathcal{H}_{all} . Right panel shows the density distribution relative to the global average, $\langle\rho\rangle_{\text{all}}$. Both panels show a slice through the midplane of a 256^3 resolution simulation with $L = 1$ Gpc.

Today (500 SNeIa $z < 0.1$)



ZTFII (3000 SNeIa $z < 0.1$)



ZTFIII (30,000 SNeIa)



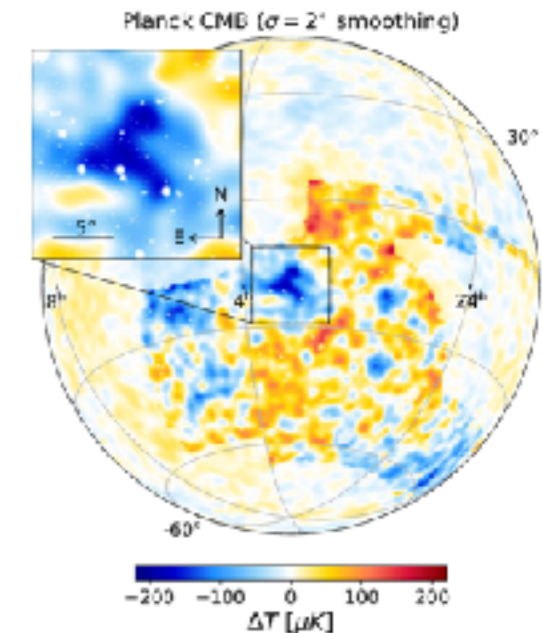
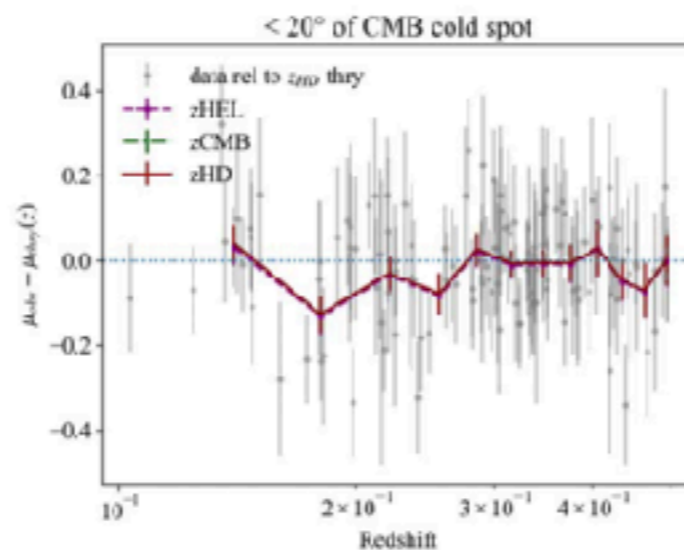
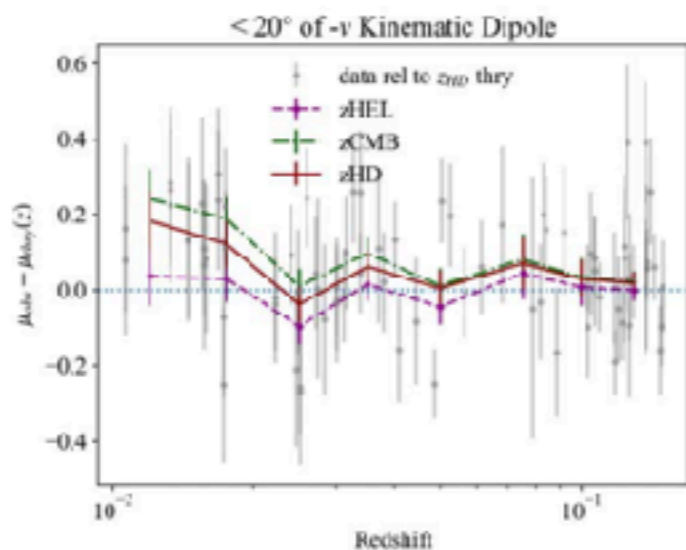
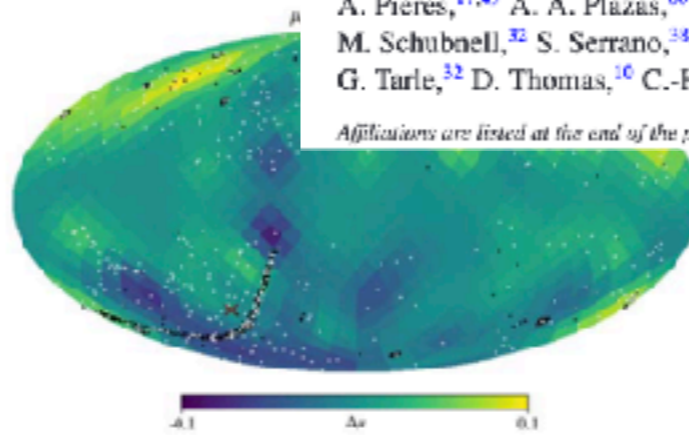
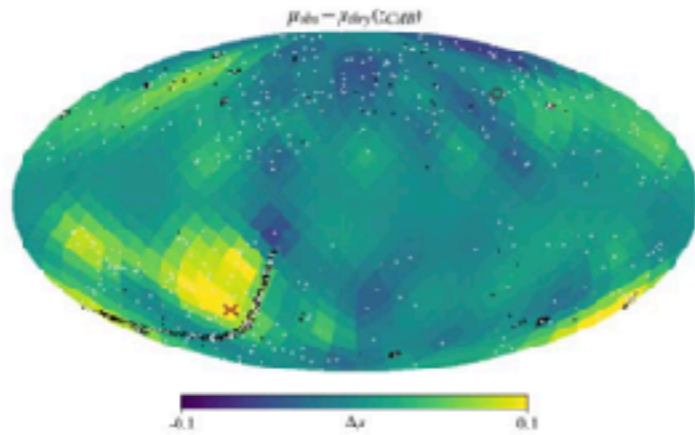
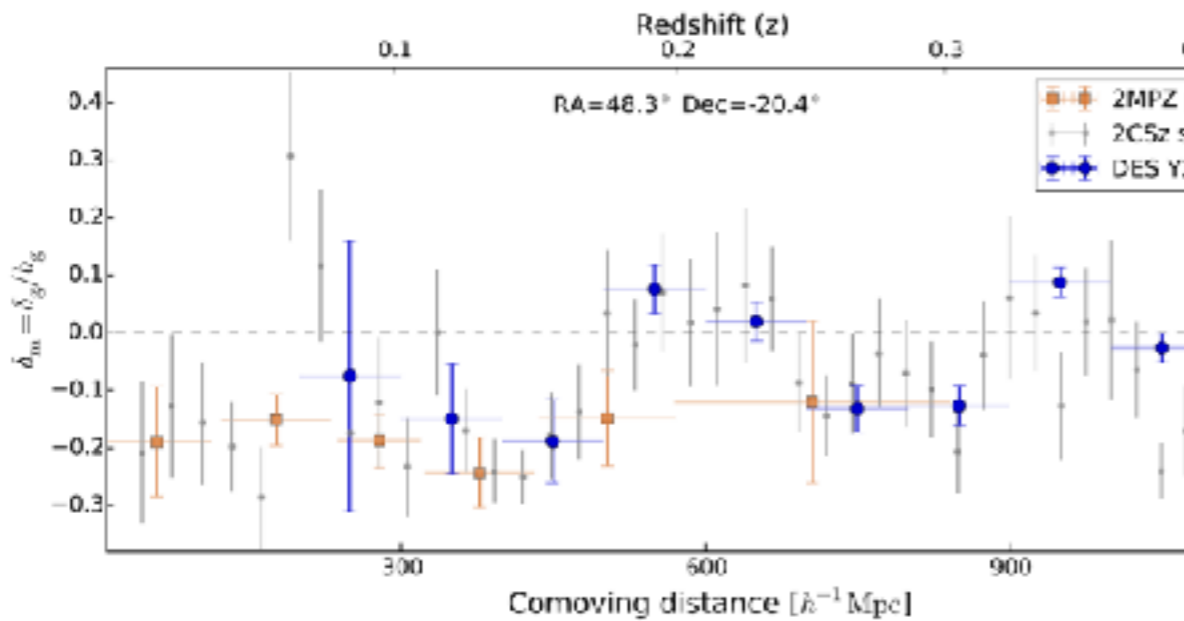
Beginning to see the sign

The DES view of the Eridanus supervoid and the CMB cold spot

A. Kovács^{1,2,*}, N. Jeffrey^{3,4}, M. Gatti^{5,6}, C. Chang^{7,8}, L. Whiteway⁴, N. Hamaus⁹, O. Lahav⁴, G. Pollina⁹, D. Bacon¹⁰, T. Kacprzak¹¹, B. Mawdsley¹⁰, S. Nadathur⁴, D. Zeurcher¹¹, J. García-Bellido¹², A. Alarcon¹³, A. Amon¹⁴, K. Bechtol¹⁵, G. M. Bernstein⁶, A. Campos¹⁶, A. Carnero Rosell^{1,2,17}, M. Carrasco Kind^{18,19}, R. Cawthon¹⁵, R. Chen²⁰, A. Choi²¹, J. Cordero²², C. Davis¹⁴, J. DeRose^{23,24}, C. Doux⁶, A. Drlica-Wagner^{7,8,25}, K. Eckert⁶, P. Elsner⁴, J. Elvin-Poole^{21,26}, S. Everett²⁴, A. Ferré²⁷, G. Giannini⁵, D. Gruen^{9,28,29}, R. A. Gruendl^{18,19}, I. Harrison^{22,30}, W. G. Hartley³¹, K. Herner²⁵, E. M. Huff²⁷, D. Hutereau³², N. Kuropatkin²⁵, M. Jarvis⁹, P. F. Leget¹⁴, N. MacCrann³³, J. McCullough¹⁴, J. Muir³⁴, J. Myles^{14,28,29}, A. Navarro-Alsina³⁵, S. Pandey⁶, J. Prat⁷, M. Raveri⁸, R. P. Rollins²², A. J. Ross²¹, E. S. Rykoff^{14,29}, C. Sánchez⁶, L. F. Seco⁶, I. Sevilla-Noarbe³⁶, E. Sheldon³⁷, T. Shin⁶, M. A. Troxel²⁰, I. Tutusaus^{38,39}, T. N. Varga^{9,40}, B. Yanny²⁵, B. Yin¹⁶, Y. Zhang²⁵, J. Zuntz⁴¹, M. Aguena^{17,42}, S. Allam²⁵, P. Andrade-Oliveira^{17,43}, J. Annis²⁵, E. Bertin^{44,45}, D. Brooks⁴, D. Burke^{14,29}, J. Carretero⁵, M. Costanzi^{46,47,48}, L. N. da Costa^{17,49}, M. E. S. Pereira³², T. Davis⁵⁰, J. De Vicente⁵⁶, S. Desai⁵¹, H. T. Diehl²⁵, I. Ferrero⁵², B. Flaugher²⁵, P. Fosalba^{38,39}, J. Frieman^{5,25}, E. Gaztañaga^{38,39}, D. Gerdes^{31,53}, T. Giannantonio^{54,55}, J. Gschwend^{17,49}, G. Gutierrez²⁵, S. Hinton⁵⁰, D. L. Hollowood²¹, K. Honscheid²¹, D. James⁵⁶, K. Kucha^{57,58}, M. Lima^{17,42}, M. A. G. Maia^{17,49}, J. L. Marshall⁵⁹, P. Melchior⁶⁰, F. Menanteau^{18,19}, R. Miquel^{5,61}, R. Morgan¹⁵, R. Ogando^{17,49}, F. Paz-Chinchon^{18,54}, A. Pieres^{17,49}, A. A. Plazas⁶⁰, M. Rodríguez Monroy²⁶, K. Romer⁶², A. Roodman^{14,29}, E. Sanchez³⁶, M. Schubnell³², S. Serrano^{38,39}, M. Smith⁶³, M. Soares-Santos³², E. Suchyta⁶⁴, M. E. C. Swanson¹⁸, G. Tarle³², D. Thomas¹⁰, C.-H. To^{14,28,29} and J. Weller^{6,40}

Affiliations are listed at the end of the paper

DES and the cold spot 217



Summary : Fact Sheet

- 150Mpc (BAO scale) represents the local universe
- All Sky Survey is needed
- σ_8 is the measure of fluctuation amplitude, σ_{100} is about 2%
- Redshift is a sum of peculiar velocity + Hubble Flow
- By using SNIa, we can extract peculiar velocity to probe local density fluctuations
- With 100 SNeIa, CMB Dipole is seen
- $z < 0.05$ SNeIa were thrown away in the past for SNIa cosmology business

Discussion ($z < 0.05$ Science)

- Peculiar Velocity = Local Density Field
- Local Density Field can be modeled
- Supergalactic Plane can be mapped
- Are we in a void?
- Local Density Map can be drawn from 10,000 SNeIa
- How do we get SNIa Spectra?
- Southern Hemisphere Facilities are needed
- Inhomogeneous Expansion of the Universe should be detectable

- Backup Slides

Local gravity versus local velocity: solutions for β and non-linear bias

Marc Davis,^{1*} Adi Nusser,² Karen L. Masters,³ Christopher Springob,⁴
John P. Huchra⁵ and Gerard Lemson⁶

¹*Departments of Astronomy & Physics, University of California, Berkeley, CA 94720, USA*

²*Physics Department and the Asher Space Science Institute-Technion, Haifa 32000, Israel*

³*Institute for Cosmology and Gravitation, University of Portsmouth, Dennis Sciama Building, Burnaby Road, Portsmouth PO1 3FX*

⁴*Anglo-Australian Observatory, PO Box 296, Epping, NSW 1710, Australia*

⁵*Harvard-Smithsonian Center for Astrophysics, 60 Garden Street, Cambridge, MA 02138, USA*

⁶*Max-Planck Institute of Astrophysics, Karl-Schwarzschild-Str. 1, 85741 Garching, Germany*

2.2 TF sample

20 yr ago, the mis-calibration of full sky Tully–Fisher (TF) data was the problem that led to very discrepant results for the determination of $\beta \equiv \Omega/b$, with $\beta = 0.5 \pm 0.2$ (DNW96) and $\beta = 1.0 \pm 0.2$ (e.g. Dekel et al. 1993). The mistaken TF calibration led to a large-scale flow that confused both analyses, but in the end, it was a calibration error in the southern sky which made a false large-scale flow (Willick et al. 1997). In one analysis, this led to a higher χ^2 than was acceptable, and in the other it led to a biased result.

$$\mathbf{v}_g(\mathbf{r}) = \frac{2f(\Omega)}{3H_0\Omega} \mathbf{g}(\mathbf{r}).$$

3.2 Peculiar velocities from the inverse Tully–Fisher relation

Given a sample of galaxies with measured circular velocity parameters, $\eta_i = \log \omega_i$, linewidth ω_i , apparent magnitudes m_i and redshifts z_i , the goal is to derive an estimate for the smooth underlying peculiar velocity field. We assume that the circular velocity parameter, η , of a galaxy is, up to a random scatter, related to its absolute magnitude, M , by means of a linear ITF relation, i.e.

$$\eta = \gamma M + \eta_0. \quad (8)$$

One of the main advantages of inverse TF methods is that samples selected by magnitude, as most are, will be minimally plagued by Malmquist bias effects when analysed in the inverse direction (Schechter 1980; Aaronson et al. 1982). We write the absolute magnitude of a galaxy,

$$M_i = M_{0i} + P_i \quad (9)$$

where

$$M_{0i} = m_i + 5 \log(z_i) - 15 \quad (10)$$

and

$$P_i = 5 \log(1 - u_i/z_i), \quad (11)$$

where m_i is the apparent magnitude of the galaxy, z_i is its redshift in units of km s^{-1} and u_i is its radial peculiar velocity in the LG frame.

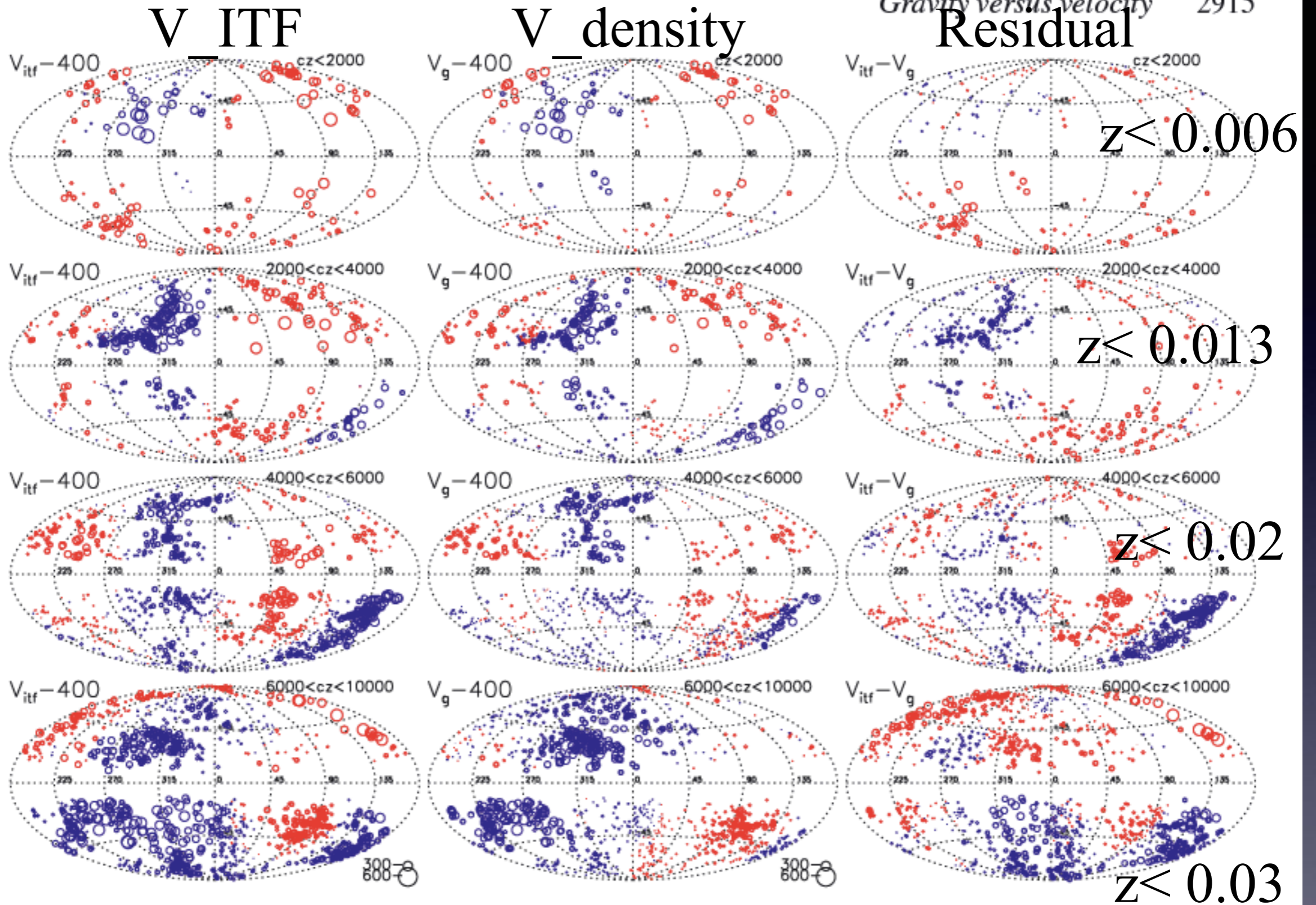


Figure 5. The derived peculiar velocities v_{ITF} , v_g and $v_{ITF} - v_g$ of galaxies on aitoff projections on the sky in galactic coordinates. The rows correspond to galaxies with $cz < 2000$, $2000 < cz < 4000$, $4000 < cz < 6000 \text{ km s}^{-1}$ and $6000 < cz < 10000 \text{ km s}^{-1}$, respectively. The size of the symbols is linearly proportional to the velocity amplitude (see key to the size of the symbols given at the bottom of the figure). In order to better see the differences, a 400 km s^{-1} dipole, in the direction of the CMB dipole, has been subtracted from the v_{ITF} and v_g velocities. Note that $v_{ITF} - v_g$ is considerably smaller than v_{ITF} or v_g , even for the most distant galaxies.

SN Ia Supernova ($z < 0.05$)

Feindt et al 2013 : SN Factory

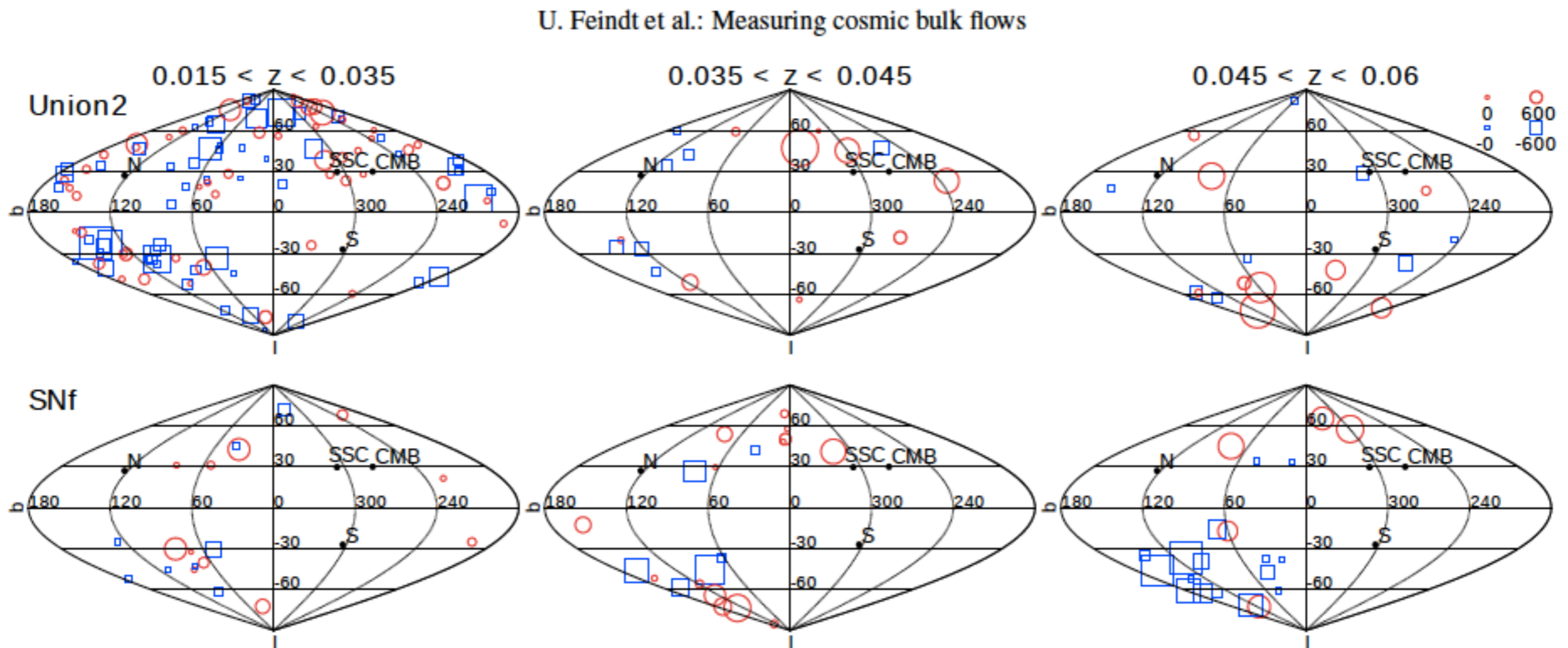


Fig. 1. Peculiar velocities of individual SNe determined from their distance moduli, μ_i , by solving Eq. (2) for v_{DF} . The plots show the Union2 (top row) and SNFACTORY (bottom row) datasets in the redshift bins $0.015 < z < 0.035$ (left column), $0.035 < z < 0.045$ (middle column) and $0.045 < z < 0.06$ (right column). The marker diameter of each SN is proportional to the absolute value of the velocity plus an offset (see the scale at the top right), with red circles corresponding to positive velocities and blue squares corresponding to negative ones. For reference, the directions of the CMB dipole and the Shapley supercluster (SSC) are shown.